Inelastic photoproduction of polarized J/ψ

M. Beneke
Theory Division, CERN, CH-1211 Geneva 23, Switzerland

M. Krämer
Rutherford Appleton Laboratory, Chilton, Didcot, OX11 0QX, England

M. Vänttinen*
NORDITA, Blegdamsvej 17, DK-2100 Copenhagen Ø, Denmark

(Received 17 September 1997; published 27 February 1998)

We study the polar and azimuthal decay angular distribution of J/ψ mesons in photoproduction experiments as functions of the inelasticity variable z and transverse momentum p_t. Future measurements of decay angular distributions at the DESY ep collider HERA will provide a new test of theoretical approaches to factorization between perturbation theory and quarkonium bound-state dynamics and shed light on the color-octet production fraction in various regions of z and p_t. [S0556-2821(98)03705-9]

PACS number(s): 13.25.Gv, 12.39.Jh, 13.60.Le

I. INTRODUCTION

The production of quarkonium in various processes, especially at high-energy colliders (for reviews, see [1,2]), has been the subject of considerable interest during the past few years. New data have been taken at $p\bar{p}$, ep and e^+e^- colliders, and a wealth of fixed-target data also exist. In theory, progress on factorization between perturbative and the quarkonium bound state dynamics has been made. The earlier ''color-singlet model'' has been superseded by a consistent and rigorous approach, based on nonrelativistic QCD (NRQCD) [3], an effective field theory that includes the so-called color-octet mechanisms. On the other hand, the ''color evaporation'' model of the early days of quarkonium physics [4] has been revived [5]. Despite these developments the range of applicability of these approaches to the practical case of charmonium is still subject to debate, as is the quantitative verification of factorization. The problematic aspect is that, because the charmonium mass is still not very large with respect to the QCD scale, nonfactorizable corrections may not be suppressed enough, if the quarkonium is not part of an isolated jet, and the expansions in NRQCD may not converge very well. In this situation cross checks between various processes, and predictions of observables such as quarkonium polarization and differential cross sections, are crucial in order to assess the importance of different quarkonium production mechanisms, as well as the limitations of a particular theoretical approach. In this paper we discuss how polar and azimuthal decay angular distributions of J/ψ, produced by real photons colliding on a proton target in the inelastic region $p_t > 1$ GeV (or, more conventionally, $z \equiv p_\psi \cdot p_p / p_\gamma \cdot p_p < 0.9$), may serve this purpose.

In the NRQCD approach, to which we adhere in this paper, the cross section for producing a charmonium state H in a photon-proton collision is written as a sum of factorizable terms,

$$d\sigma(H) = \sum_{i,j \in \{q,g,\gamma\}} \int dx_1 dx_2 f_{i/\gamma}(x_1) f_{j/p}(x_2) \times \sum_n d\hat{\sigma}(i+j \to c\bar{c}[n]) \langle \mathcal{O}_n^H \rangle, \quad (1)$$

where n denotes the color, spin and angular momentum state of an intermediate $c\bar{c}$ pair and $f_{i/\gamma}$ and $f_{j/p}$ the parton distributions in the photon and the proton, respectively. The short-distance cross sections $d\hat{\sigma}(i+j \to c\bar{c}[n])$ can be calculated perturbatively in the strong coupling α_s. The matrix elements $\langle \mathcal{O}_n^H \rangle \equiv \langle 0 | \mathcal{O}_n^H | 0 \rangle$ (see [3] for their definition) are related to the nonperturbative transition probabilities from the $c\bar{c}$ state n into the quarkonium H. The magnitude of these probabilities is determined by the intrinsic velocity v of the bound state. Thus the above sum is a double expansion in α_s and v.

Within NRQCD the leading term in v to inelastic photoproduction of J/ψ comes from an intermediate $c\bar{c}$ pair in a color-singlet ${}^3S_1$ state and coincides with the color-singlet model result. (The notation for the angular momentum configuration is ${}^{2S+1}L_J$ with S, L and J denoting spin, orbital and total angular momentum, respectively.) Cross sections [6], polar [7], and polar and azimuthal [8] decay angular distributions have been calculated for the direct-photon contribution, in which case $i = \gamma$ and $f_{\gamma/\gamma}(x) = \delta(1-x)$ in (1). The angular integrated cross section is known to next-to-leading order (NLO) in α_s [9]. The color-singlet contribution, including next-to-leading corrections in α_s, is known to reproduce the unpolarized data adequately. But there is still a considerable amount of uncertainty in the normalization of the theoretical prediction, which arises from the value of the charm quark mass and the wave function at the origin, as well as the choice of parton distribution functions and renormalization or factorization scale.

*Present address: Institut für Theoretische Physik, Physik-Department der Technischen Universität München, 85747 Garching, Germany.

At order $v^4 \sim 0.05-0.1$ relative to the color-singlet contribution, the J/ψ can also be produced through intermediate color-octet $^3S_1$, $^1S_0$ and ^3P_J configurations. In the inelastic region, they have been considered in [10,11] for the direct photon contribution and in [12] for resolved photons, in which case the photon participates in the hard scattering through its parton content. Color-octet contributions to the total photoproduction cross section (integrated over all z and p_t) are known to next-to-leading order [13]. The polarization of inelastically produced J/ψ due to these additional production mechanisms, however, has not been calculated so far.

Because the color-octet contributions are suppressed as v^4, but, in the inelastic region, contribute at the same order in α_s as the color-singlet contribution, they are of interest only if they are enhanced by other factors, either numerical or kinematical. In this respect the situation is similar to a certain v^2 correction, which arises already in the color-singlet model [14] and becomes kinematically enhanced at z close to 1. The color-octet production channels are indeed kinematically different from the color-singlet one, because the $^1S_0$ and ^3P_J configurations can be produced through t-channel exchange of a gluon already at lowest order in α_s. (For the $^3S_1$ octet this is true for the resolved process.) This leads to a significantly enhanced amplitude, in particular in the large-z region. The color-octet contributions to J/ψ photoproduction are indeed strongly peaked at large z [10,11]. Such a shape is not supported by the data, which at first sight could lead to a rather stringent constraint on the octet matrix elements $\langle \mathcal{O}_8[n] \rangle$, $n \in \{^1S_0, ^3P_0\}$ and to an inconsistency with the values obtained for these matrix elements from other processes. However, the peaked shape of the z distribution is derived neglecting the energy transfer in the nonperturbative transition $c\bar{c}[n] \to J/\psi + X$. In reality the peak may be considerably smeared [15] as a consequence of resuming kinematically enhanced higher-order corrections in v^2 and no constraint or inconsistency can be derived from the endpoint behavior of the z distribution at present. As a consequence, the role of octet contributions to the direct process remains unclear. The resolved photon contribution, on the other hand, could be entirely color-octet dominated [12,16]. The z distribution should then begin to rise again at small z, if the color-octet matrix elements are as large as suggested by NRQCD velocity scaling rules [17,3] and fits to hadroproduction data.

Our motivation for considering the decay angular distributions, including all direct and resolved production mechanisms, is to provide another observable that can clarify the relative importance of color-octet production in photoproduction in different kinematic regions. Many of the abovementioned uncertainties and difficulties do not affect the polarization yield. For example, the resummation that is necessary in the endpoint region may lead to a significant redistribution of $d\sigma/dz$ in z, but affects the normalized decay angular distributions to a lesser degree, if they do not have a strong z dependence in the region affected by the smearing. We find that some angular coefficients, especially those for the azimuthal angle dependence, take essentially different values in the color-singlet and color-octet processes. A measurement of decay angular distributions would therefore provide information on the relevance of color-octet production, also at z close to 1, which is largely independent of normalization uncertainties.

The polarization of the J/ψ can be determined by measuring the angular distribution of the leptonic decay $J/\psi \to l^+ l^-$. To date, experimental measurements of J/ψ polarization exist only for diffractive (elastic and proton dissociation) photoproduction [18,19], to which the inclusive formalism of NRQCD does not apply, and for fixed-target hadroproduction [20]. The latter can be compared with predictions obtained in the color-singlet model [21] and NRQCD [22,23] for p_t-integrated cross sections. As discussed in [2] the experimental finding of no polarization is only marginally consistent with the NRQCD prediction. Photoproduction offers another opportunity to learn about whether the J/ψ polarization carries information on the spin of the heavy quark pair produced at short distances, which is expected in theoretical approaches in which spin symmetry is at work. With the expected increase in luminosity at the DESY ep collider HERA, polarization in photoproduction of J/ψ at different values of z and p_t could provide an attractive diagnostic tool in addition to the widely discussed polarization measurement in $p\bar{p}$ collisions at the Fermilab Tevatron [24–27].

The paper is organized as follows: Sec. II discusses the production mechanisms and calculational details regarding decay angular distributions. In Sec. III we pause for theoretical considerations that influence our choice of cuts and other parameters in the analysis. Section IV presents results and their discussion, followed by a summary in Sec. V. Appendix A contains the covariant definitions of coordinate systems and polarization vectors and Appendix B summarizes the density matrices for all subprocesses considered in the paper.

II. PRODUCTION MECHANISMS AND CROSS SECTIONS

We assume that the J/ψ transverse momentum $p_t > 1$ GeV, in order to suppress the diffractive contribution and higher-twist corrections in general. Away from $p_t = 0$ (or $z = 1$) the leading-twist hard subprocesses contributing to inelastic J/ψ production can be classified as follows.

(1) Direct photon mechanisms. At leading order in the strong coupling constant, $O(\alpha \alpha_s^2)$, these are

$$\gamma + g \to c\bar{c}[^3S_1^{(1)}, ^3S_1^{(8)}, ^1S_0^{(8)}, ^3P_J^{(8)}] + g, \tag{2}$$

$$\gamma + q/\bar{q} \to c\bar{c}[^3S_1^{(8)}, ^1S_0^{(8)}, ^3P_J^{(8)}] + q/\bar{q}, \tag{3}$$

where the initial-state parton originates from the target proton.

(2) Resolved photon mechanisms. At leading order, $O(\alpha_s^3)$, the subprocesses are

$$g + g \to c\bar{c}[^3S_1^{(1)}, ^3S_1^{(8)}, ^1S_0^{(8)}, ^3P_J^{(8)}] + g, \tag{4}$$

$$g + q/\bar{q} \to c\bar{c}[^3S_1^{(8)}, ^1S_0^{(8)}, ^3P_J^{(8)}] + q/\bar{q}, \tag{5}$$

$$q+\overline{q}\to c\overline{c}[^3S_1^{(8)},{}^1S_0^{(8)},{}^3P_J^{(8)}]+g, \tag{6}$$

where one of the initial-state partons originates from the photon and the other originates from the proton.

The direct-photon mechanisms dominate in the region $z \gtrsim 0.2$, whereas resolved-photon mechanisms become important in the region $z \lesssim 0.2$. (These numbers depend on the values of the color-octet matrix elements, as well as on the p_t cut.) At HERA energies, photon-quark fusion can contribute about 10–15 % to the cross section at large z. Quark-gluon fusion constitutes about 20–40 % of the resolved cross section at $z \lesssim 0.2$ and becomes more important than gluon-gluon fusion at larger z. Quark-antiquark fusion is always completely negligible.

The above list includes those color-octet production channels that are suppressed by at most v^4 relative to the leading color singlet production channel. The suppression of the octet contributions follows from a multipole expansion of the nonperturbative transition $c\overline{c}[n]\to J/\psi+X$. From a $^3P_J^{(8)}$ intermediate state, the physical J/ψ state can be reached by a single chromoelectric dipole transition, from a $^3S_1^{(8)}$ state by two consecutive electric dipole transitions, and from a $^1S_0^{(8)}$ state by a chromomagnetic dipole transition. Each electric dipole transition brings a factor v^2, and the magnetic dipole transition a factor v^4. In addition, the hard production vertex for a P-wave $c\overline{c}$ state is suppressed already by v^2 relative to production in an S-wave state. In photon-gluon fusion, the $^3S_1^{(8)}$ amplitude is kinematically identical to the $^3S_1^{(1)}$ amplitude. The $^3S_1^{(8)}$ channel is therefore insignificant for the direct-photon contribution.

In resolved photon interactions, on the other hand, the $^3S_1^{(8)}$ channel dominates at $p_t \gtrsim 5$ GeV, because it includes a gluon fragmentation component [28], in both the gluon-gluon and gluon-quark fusion contributions, and therefore falls only as $1/p_t^4$ at large p_t. The resolved photon amplitudes are identical to those relevant to J/ψ production in hadron-hadron collisions [29,26] and at HERA energies the relative importance of the various contributions as functions of p_t is nearly the same as at Tevatron energies.

The direct-photon mechanisms above all decrease at least as $1/p_t^6$ at large p_t, with the exception of $\gamma+q\to c\overline{c}[^3S_1^{(8)}]+q$. Fragmentation contributions in photon-gluon fusion exist only at the next order in α_s. They exceed the leading-order contributions at $p_t \gtrsim 10$ GeV [30,16]. We therefore conclude that our list includes all important leading-twist production mechanisms for all z and as long as $p_t \lesssim 10$ GeV.

We expect that higher-twist corrections due to multiple interactions with the proton or photon remnant would be suppressed as a power of $\Lambda^2/(Q^2+p_t^2)$, where $\Lambda \lesssim 1$ GeV is a typical QCD scale and Q is one of the scales involved in the bound state dynamics, $Q \approx m_c$, $m_c v$, or $m_c v^2$. Since $mv^2 \sim \Lambda$ for charmonium and bottomonium, one may expect large higher-twist corrections at small p_t, when the heavy quark-antiquark pair moves parallel with a remnant jet and remains in its hadronization region over a time $1/\Lambda$ in the quarkonium rest frame.[1]

The differential cross section for J/ψ production and its subsequent leptonic decay $J/\psi\to l^+l^-$ through any of the resolved-photon subprocesses can be written as

$$\frac{1}{B_{ll}}\frac{d\sigma^{ij}}{d\Omega\, dz\, dp_t}=\int_{x_1,\min}^1 dx_1 f_{i/\gamma}(x_1,\mu_F) f_{j/p}(x_2,\mu_F)\,\frac{1}{16\pi\hat{s}^2}\,\frac{2x_1x_2p_t}{z(x_1-z)}\,\frac{3}{8\pi}\,[\rho_{11}^{ij}+\rho_{00}^{ij}+(\rho_{11}^{ij}-\rho_{00}^{ij})\cos^2\theta$$

$$+\sqrt{2}\,\mathrm{Re}(\rho_{10}^{ij})\sin 2\theta\cos\phi+\rho_{1,-1}^{ij}\sin^2\theta\cos 2\phi], \tag{7}$$

where B_{ll} is the $J/\psi\to l^+l^-$ branching ratio, $s=(p_\gamma+p_p)^2$, $\hat{s}=x_1x_2s$ and the parton distribution of the proton is evaluated at

$$x_2=\frac{x_1p_t^2+M^2(x_1-z)}{sz(x_1-z)} \tag{8}$$

with factorization scale μ_F. Here and in the following we use $M=2m_c$. The variables z and p_t are subject to the restriction

$$(1-z)(sz-M^2)>p_t^2 \tag{9}$$

and

$$x_1>x_{1,\min}=\frac{z(sz-M^2)}{sz-p_t^2-M^2}. \tag{10}$$

The angles θ and ϕ refer to the polar and azimuthal angle of

[1]Some aspects of higher-twist corrections to $\gamma+g\to c\overline{c}[^3S_1^{(1)}]+g$ have been considered in [31], with the surprising conclusion that the higher-twist correction is $\Lambda^2/(4m_c^2)$, even at very large p_t, rather than Λ^2/p_t^2. The term that does not scale as Λ^2/p_t^2 enters in the combination $e_1(z)+4d_1(z)$, where e_1 and d_1 are certain twist-4 multiparton correlation functions defined in [31]. However, in the approximation considered in [31] one finds $e_1=4d_1$. If there existed a sign inconsistency in [31], the $\Lambda^2/(4m_c^2)$ term would disappear and the result conform to our intuition.

the l^+ in the J/ψ decay with respect to a coordinate system defined in the J/ψ rest frame. (See Appendix A for details on their definition.) Finally

$$\rho^{ij}_{\lambda\lambda'} \equiv A[ij\to J/\psi(\lambda)+X]A^*[ij\to J/\psi(\lambda')+X] \quad (11)$$

are density matrix elements for J/ψ production, where a summation (average) over the spins of $X(i,j)$ is understood. The kinematical relations for the direct-photon process follow from setting $i=\gamma$ and $f_{\gamma/\gamma}(x_1,\mu_F)=\delta(1-x_1)$.

The polarization analysis in NRQCD [25,23,32] is based on the symmetries of the NRQCD Lagrangian, of which spin and rotational symmetry are crucial. In electric dipole transitions the heavy quark spins remain intact, so that the J/ψ spin orientation will be the same as the perturbatively calculable orientation of the total $c\bar{c}$ spin $s_q+s_{\bar{q}}$ in the intermediate state. The ${}^1S_0^{(8)}$ intermediate state is rotationally invariant and leads to random orientation of the J/ψ spin. Technically, we have

$$\rho^{ij}_{\lambda\lambda'} = \rho^{ij}_{\lambda\lambda'}[{}^3S_1^{(1)}] + \rho^{ij}_{\lambda\lambda'}[{}^3S_1^{(8)}] + \rho^{ij}_{\lambda\lambda'}[{}^1S_0^{(8)}] + \rho^{ij}_{\lambda\lambda'}[\{S=1,L=1\}^{(8)}] + \cdots , \quad (12)$$

where $\rho^{ij}_{\lambda\lambda'}[n]$ refers to production through a $c\bar{c}$ pair in a state n. The above decomposition implies that no interference occurs between the amplitudes for the different terms in the sum. The symmetries of NRQCD do not forbid interference of different ${}^3P_J$ states. One finds [25]

$$\rho^{ij}_{\lambda\lambda'}[\{S=1,L=1\}^{(8)}] \propto \sum_{L_z} A[ij\to c\bar{c}(1L_z;1\lambda)]+X] \times A^*[ij\to c\bar{c}[(1L_z;1\lambda')]+X] \neq \sum_{J=0,1,2} \rho^{ij}_{\lambda\lambda'}[{}^3P_J^{(8)}], \quad (13)$$

where the quantum numbers of the $c\bar{c}$ pair refer to (LL_z,SS_z). NRQCD factorization implies that the density matrices can be written as

$$\rho^{ij}_{\lambda\lambda'}[n] = K^{ij}[n]_{ab\ldots}\langle \mathcal{O}^{J/\psi}_{\lambda\lambda'}[n]_{ab\ldots}\rangle, \quad (14)$$

where $\langle \mathcal{O}^{J/\psi}_{\lambda\lambda'}[n]_{ab\ldots}\rangle$ is a NRQCD matrix element with Cartesian indices $a,b,\ldots$, and $K^{ij}[n]_{ab\ldots}$ the corresponding short-distance coefficient. The final step is a tensor decomposition of these matrix elements, which, in the case of interest, can be formulated as a projection of the $c\bar{c}$ production amplitude. For J/ψ production at the considered order in v^2, the symmetries of NRQCD are sufficient to reduce all nonperturbative input to the four parameters $\langle \mathcal{O}^{J/\psi}[n]\rangle$ with $n \in \{{}^3S_1^{(1)}, {}^3S_1^{(8)}, {}^1S_0^{(8)}, {}^3P_0^{(8)}\}$ defined as for *unpolarized* J/ψ production.

The calculation then consists of evaluating the density matrix elements for each separate term in (12) and all partonic subprocesses. We express these matrices as

$$\begin{aligned}\rho^{ij}_{\lambda\lambda'}[n] = {} & A^{ij}[n][\epsilon^*(\lambda)\cdot\epsilon(\lambda')] \\ & + M^2 B^{ij}[n][p_1\cdot\epsilon^*(\lambda)p_1\cdot\epsilon(\lambda')] \\ & + M^2 C^{ij}[n][p_2\cdot\epsilon^*(\lambda)p_2\cdot\epsilon(\lambda')] \\ & + M^2 D^{ij}[n][p_1\cdot\epsilon^*(\lambda)p_2\cdot\epsilon^*(\lambda') \\ & + p_2\cdot\epsilon^*(\lambda)p_1\cdot\epsilon(\lambda')], \end{aligned} \quad (15)$$

where $\epsilon(\lambda)$ is the J/ψ polarization vector, p_1 is the momentum of the photon (or the parton originating from the photon in resolved contributions), and p_2 is the momentum of the parton in the target. The coefficients A,B,C,D are independent of the choice of axes in the J/ψ rest frame and proportional to a NRQCD matrix element. Their analytic expressions are collected in Appendix B.

The decay angular distribution in the J/ψ rest frame is often parametrized as

$$\frac{d\sigma}{d\Omega dy} \propto 1+\lambda(y)\cos^2\theta + \mu(y)\sin 2\theta\cos\phi + \frac{\nu(y)}{2}\sin^2\theta\cos 2\phi, \quad (16)$$

where y stands for a set of variables and λ, μ, ν are obviously related to (appropriate integrals of) the density matrix elements as

$$\lambda = \frac{\rho_{11}-\rho_{00}}{\rho_{11}+\rho_{00}}, \quad \mu = \frac{\sqrt{2}\ \mathrm{Re}\ \rho_{10}}{\rho_{11}+\rho_{00}}, \quad \nu = \frac{2\rho_{1,-1}}{\rho_{11}+\rho_{00}}. \quad (17)$$

Because of the dependence of $\epsilon(\lambda)$ on the definition of a coordinate system (see Appendix A), the parameters λ, μ, ν depend on this definition.

III. THEORETICAL CONSIDERATIONS

In this section we discuss some theoretical issues that influence our choice of cuts. We also motivate the values of NRQCD long-distance matrix elements that we subsequently use.

The NRQCD expansion of the quarkonium production cross section applies to the leading-twist contribution of an inclusive production cross section. Leading-twist means that the result is accurate up to corrections that scale as some power of Λ/m_c in the limit that $m_c\to\infty$. Up to such corrections, NRQCD also applies to the total J/ψ photoproduction cross section. The leading contribution is $O(\alpha\alpha_s)$ and purely colour-octet [10,33]. It formally contributes only at $z=1$, $p_t=0$, i.e., in the diffractive region. Soft-gluon emission during conversion of the color-octet $c\bar{c}$ pair into a J/ψ is expected to ''smear'' the delta functions at $z=1$ and $p_t=0$ over a region $\delta z\sim 0.25$, $\delta p_t\sim 0.5$ GeV [15]. One may ask whether the experimentally measured diffractive J/ψ cross section (with or without proton dissociation) could be considered as part of the leading-twist total cross section. Or

whether it should be considered as a pure higher-twist phenomenon which cannot be regarded as dual (in the sense of parton-hadron duality) to the $O(\alpha\alpha_s)$ contribution in the inclusive formalism.

In order for the first possibility to be realized, the soft gluons, which are emitted in the transition of the color-octet $c\bar{c}$ pair into $J/\psi+X$, would have to recombine into a proton or a low-mass diffractive final state. Although it cannot be argued from first principles against this possibility, it certainly appears unlikely. It would also hardly be compatible with the factorization assumption of NRQCD that the above color neutralization is universal, i.e., independent of the rest of the process, again up to higher-twist corrections. (Clearly, complete independence is not possible, because some color exchange between $J/\psi+X$ and the rest of the process is necessary, if the $J/\psi+X$ state originates from a color-octet $c\bar{c}$ pair.)

The clearest indication that the diffractive contribution should be considered as a higher-twist correction, which is not part of a leading-twist calculation of NRQCD, is experimental. The H1 Collaboration has measured [18] the polar decay angle distribution and the ZEUS Collaboration has measured [19] the polar and azimuthal decay angular distribution. Models of diffractive production based on hard two-gluon [34,35] or soft-Pomeron [36] exchange predict $\lambda=1$ [34] [λ is defined in [16]], in agreement with the HERA measurements and earlier fixed-target data [37]. On the other hand, the polarization signature of the leading-twist parton reaction $\gamma g\to c\bar{c}$ is identical to the signature in the process $gg\to c\bar{c}$ [23]. The result is $\lambda=0$ if the $^1S_0$ configuration dominates and $\lambda=1/2$ if ^3P_J dominates. Any linear combination of these values is incompatible with the experimental data. Since the diffractive cross section (according to the experimental definitions of [18,19]) is about as large as the inelastic cross section [18,38], we conclude that NRQCD cannot be used to predict the photoproduction cross section integrated over all z and p_t.

In order to apply NRQCD we therefore have to cut the elastic region without restricting the inclusive nature of the process. The HERA collaborations conventionally define the inelastic region through the requirement $z<0.9$. Let us now argue that it is theoretically advantageous to define the inelastic region through a cut in p_t. It is obvious theoretically, and confirmed experimentally, that the slope of the p_t distribution is significantly smaller for inelastic production than for elastic production (with or without proton dissociation). A p_t cut at $p_t>1$ GeV already eliminates most of the diffractive contribution as well as higher-twist corrections in general and no further cut on z is necessary. In fact, the cross section with an additional cut $z<0.9$ *cannot* be reliably predicted in NRQCD. As emphasized in [15], because the NRQCD expansion is singular at $z=1$, only an average cross section over a sufficiently large region close to $z=1$ can be predicted. The z distribution itself requires additional nonperturbative information in the form of so-called shape functions. These shape functions are also required to predict the p_t distribution with an additional cut $z<0.9$, but not if z is integrated up to its kinematic maximum. In the following, we define the inelastic region through the cut $p_t>1$ GeV. If statistics is not a limitation, it might be preferable to use $p_t>2$ GeV to further suppress the higher-twist contributions and difficulties in predicting the p_t distribution at low p_t, because of (perturbative) soft-gluon emission. Note that the resummation of higher-order v^2 corrections in NRQCD will also cause some smearing in transverse momentum, which we expect to be less important than that caused by perturbative soft-gluon emission.

Because the color-octet contributions to inelastic J/ψ production are strongly enhanced at large z, an immediate consequence of integrating up to $z_{\max}$ rather than 0.9 is that the p_t distribution is now dominated by color-octet production, as will be discussed in more detail below. The suggested importance of the color-octet mechanisms could be further investigated experimentally, if hadronic activity in the vicinity of the J/ψ could be detected. If a J/ψ is produced through a color-octet $c\bar{c}$ pair, we expect it to be accompanied by light hadrons more often than if it is produced through a color-singlet pair.

The cross sections and decay angular distributions depend on four parameters related to the probability of the transition $c\bar{c}[n]\to J/\psi+X$. The color singlet matrix element can be related to the J/ψ wave function at the origin. For $\langle\mathcal{O}_8^{J/\psi}(^3S_1)\rangle$ we use the value obtained in [26] from a fit to hadroproduction of J/ψ at large p_t. Its precise numerical value does not influence our analysis, because the $^3S_1$-color-octet channel is important only for resolved photons at large transverse momentum. Our predictions do depend crucially on $\langle\mathcal{O}_8^{J/\psi}(^1S_0)\rangle$ and $\langle\mathcal{O}_8^{J/\psi}(^3P_0)\rangle$, both of which are not very well known. The following constraints can be obtained from other J/ψ production processes:

$$\langle\mathcal{O}_8^{J/\psi}(^1S_0)\rangle+\frac{3.5}{m_c^2}\langle\mathcal{O}_8^{J/\psi}(^3P_0)\rangle=(3.90\pm1.14)\times10^{-2}\ \text{GeV}^3\quad(\text{Tevatron [26]})$$

$$\langle\mathcal{O}_8^{J/\psi}(^1S_0)\rangle+\frac{7}{m_c^2}\langle\mathcal{O}_8^{J/\psi}(^3P_0)\rangle=3.0\times10^{-2}\ \text{GeV}^3\quad(\text{fixed-target hadroproduction [23]})$$

$$\langle\mathcal{O}_8^{J/\psi}(^1S_0)\rangle+\frac{3.6}{m_c^2}\langle\mathcal{O}_8^{J/\psi}(^3P_0)\rangle<2.8\times10^{-2}\ \text{GeV}^3\quad(B\to J/\psi X)$$

TABLE I. Values of the NRQCD matrix elements in 10^{-2} GeV^3 taken for the analysis; $m_c = 1.5$ GeV.

Scenario	$\langle \mathcal{O}_1^{J/\psi}(^3S_1)\rangle$	$\langle \mathcal{O}_8^{J/\psi}(^3S_1)\rangle$	$\langle \mathcal{O}_8^{J/\psi}(^1S_0)\rangle$	$\langle \mathcal{O}_8^{J/\psi}(^3P_0)\rangle/m_c^2$
I	116	1.06	3.0	0.0
II	116	1.06	0.0	1.0

where $m_c = 1.5$ GeV is assumed. For various reasons, all of these determinations should probably be considered as uncertain within a factor of 2. The constraint from inclusive B decays has been obtained from the leading-order calculation of [11,39], setting the color-singlet contribution, whose magnitude is rather uncertain, to zero. (With the parameters of [39], we would have obtained 4.4×10^{-2} GeV^3 instead of 2.8×10^{-2} GeV^3.) Including the color-singlet contribution would strengthen the inequality considerably, but this cannot be justified given the NLO result of [40]. In view of these uncertainties and given that they do not allow us to constrain separately $\langle \mathcal{O}_8^{J/\psi}(^1S_0)\rangle$ and $\langle \mathcal{O}_8^{J/\psi}(^3P_0)\rangle$ with confidence, we consider two scenarios in which the constraints are (approximately) saturated either by $\langle \mathcal{O}_8^{J/\psi}(^1S_0)\rangle$ or $\langle \mathcal{O}_8^{J/\psi}(^3P_0)\rangle$ alone.

The values of all parameters are summarized in Table I. Further constraints could be obtained from the p_t distribution in photoproduction, if all kinematically allowed z are integrated over. However, for the reasons mentioned earlier, no constraint can be derived from the endpoint region of the z distribution.

IV. RESULTS

A. Cross sections

We begin with differential cross sections in order to display the relative magnitude of the various contributions, whose different polarization yield will influence the decay angular distributions.

The J/ψ energy distribution is shown in Fig. 1 as a function of the scaling variable $z = p_\psi \cdot p_p / p_\gamma \cdot p_p$ for a typical HERA photon-proton center-of-mass energy $\sqrt{s_{\gamma p}} = 100$ GeV and compared with H1 [18] and ZEUS [38] data. (Apart from slightly different color-octet matrix elements, the presentation coincides with that of [12].) The color-octet contributions exceed the color-singlet contribution both for large $z \gtrsim 0.65$ and for small $z \lesssim 0.25$.

The normalization of the short-distance cross sections is strongly affected by the choice of the charm quark mass, the QCD coupling, the renormalization/factorization scale μ, and the parton distribution functions. Varying the parameters in the range $1.35\ \text{GeV} < m_c < 1.65$ GeV, $m_c < \mu < 4m_c$, and $150\ \text{MeV} < \Lambda^{(4)} < 250$ MeV, the normalization of $d\hat{\sigma}(ij \to c\bar{c}[n])$ is altered by $\sim \pm 50\%$ around the central value[2] at $m_c = 1.5$ GeV, $\mu = 2m_c$, and $\Lambda^{(4)} = 200$ MeV. Adopting, e.g., the Martin-Roberts-Stirling set R2 [MRS (R2)] set of parton distributions [43] and the corresponding value of α_s decreases the short-distance cross sections by about a factor of 2 as compared to the leading-order Glück-Reya-Vogt (GRV) parametrization. However, the values of the nonperturbative color-octet matrix elements as extracted from fits to the Tevatron data [26] depend on the choice of m_c, α_s, μ and the parton distribution in approximately the opposite way such as to compensate the change in the short-distance cross section. At leading-twist and leading order in α_s, the overall normalization uncertainty of the color-octet contributions to J/ψ photoproduction is thus in the range of only about $\pm 10\%$, if the short-distance cross sections are multiplied with nonperturbative matrix elements that have been extracted from hadroproduction data using the same set of input parameters. The long-distance factor of the color-singlet cross section $\langle \mathcal{O}_1^{J/\psi}(^3S_1)\rangle$ on the other hand can be determined from the leptonic decay width and is not very sensitive to the choice of parameters, up to unknown contributions from next-to-next-to-leading-order QCD corrections. Consequently, the normalization uncertainty of the short-distance cross section $d\hat{\sigma}(ij \to c\bar{c}[^3S_1^{(1)}])$ is not compensated by a change in the long-distance factor and the color-singlet contribution should be considered uncertain within a factor of two. Next-to-leading order QCD corrections [9] increase the color-singlet cross section by $\sim 20-40\,\%$, depending in detail on the choice of parameters, but do not affect the shape of the J/ψ energy distribution.

Given the large normalization uncertainties in particular of the color-singlet contribution, no conclusive statement about the size of the color-octet matrix elements can be derived from the J/ψ energy distribution in the region $z \lesssim 0.8$. On the other hand, the dramatic increase of the color-octet cross section at larger z is not supported by the data. One should not interpret this discrepancy as a failure of the NRQCD theory itself, but rather as an artifact of our leading-order approximation in α_s and v^2 for the color-octet contributions. Close to the boundary of phase space, for $z \gtrsim 0.75$, the shape of the z distribution cannot be predicted without resumming singular higher-order terms in the velocity expansion [15]. This difficulty is exactly analogous to the well-known problem of extracting the Cabibbo-Kobayashi-Maskowa (CKM) matrix element $|V_{ub}|$ from the endpoint region of the lepton energy distribution in semileptonic B decay. To constrain the color-octet contributions from the J/ψ z distribution, the distribution would have to be averaged close to the endpoint over a region *much larger* than $v^2 \sim 0.25$.

The low-z region is not expected to be sensitive to higher-order terms in the velocity expansion. Therefore, if the data could be extended to the low-z region, an important resolved photon contribution should be visible, if the color-octet matrix elements are not significantly smaller than assumed in Table I.

The p_t distribution for inelastically produced J/ψ is shown in Fig. 2 with a lower z cut: $z > 0.1$. As discussed in Sec. III no upper cut in z is necessary or advisable to suppress the diffractive contribution, if the transverse momentum is above about 1 GeV. With this definition the differential cross section is dominated by color-octet contributions, which exceed the color-singlet contribution by almost an order of magnitude, similar to their significance in hadron-hadron collisions at fixed-target energies [23]. Experimental

[2]To study the α_s dependence of the cross section, we use consistently adjusted sets of parton densities [41,42].

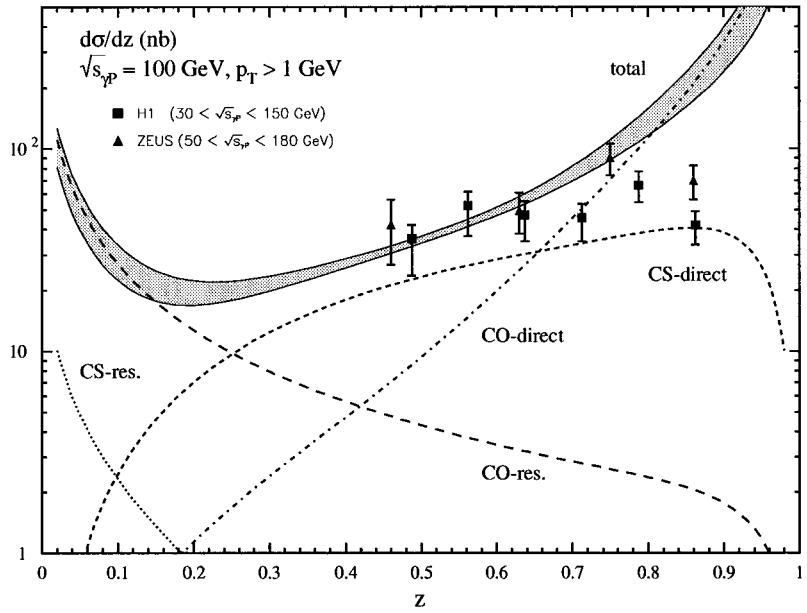

FIG. 1. Color-singlet (CS) and color-octet (CO) contributions due to direct and resolved photons to the J/ψ energy distribution $d\sigma/dz$ at the photon-proton center-of-mass energy $\sqrt{s_{\gamma p}}=100\,\mathrm{GeV}$ in comparison with HERA data [18,38] averaged over the specified range of $\sqrt{s_{\gamma p}}$. The shaded area bounded by the solid lines represents the sum of all contributions according to scenarios I and II for the color-octet matrix elements. The lines corresponding to separate color-octet contributions are plotted for $\langle\mathcal{O}_8^{J/\psi}(^1S_0)\rangle=\langle\mathcal{O}_8^{J/\psi}(^3P_0)\rangle/m_c^2=0.008\ \ \mathrm{GeV}^3$. The color-singlet cross section is evaluated in leading order in α_s. Other parameters: $m_c=1.5\,\mathrm{GeV}$, renormalization/factorization scale $\mu=2m_c$, GRV LO proton and photon parton distributions [41], $\Lambda_{LO}^{(4)}=200$ MeV.

data from HERA exist only for $p_t<3$ GeV [18,38]. The data are presented with a cut at $z<0.9$, in which case the differential cross section at $p_t=1$ GeV (3 GeV) is found to be about a factor of 10 (2) smaller than in Fig. 2. The transverse momentum distribution at $z<0.9$ is adequately accounted for by the color-singlet channel, including next-to-leading-order corrections in α_s [9]. Diagrams with t-channel gluon exchange lead to large K factors that increase with increasing transverse momentum and harden the p_t-spectrum of the color-singlet channel at NLO considerably. We do not expect a similar strong impact of next-to-leading order QCD corrections on the transverse momentum distribution of the color-octet cross sections. It would be interesting to learn whether including all z can lead to stringent constraints on the size of the color-octet matrix elements. However, in order to obtain an accurate theoretical prediction in the lower-p_t region, $p_t\lesssim 2-3\,\mathrm{GeV}$, perturbative soft-gluon resummation would have to be taken into account. We expect that soft-gluon resummation will be more important for the color-octet processes, because there is no Sudakov form factor for radiation off the $c\bar{c}$ pair in the color-singlet $^3S_1$ channel, for which there exists a color dipole moment only.

B. Decay angular distributions

We now turn to the decay angular distributions, which constitute the main result of this work. Below we present the z and p_t dependence of the polar and azimuthal decay angular distribution parameters λ, μ, ν defined in (16), at a typical HERA center-of-mass energy of $\sqrt{s}=100\,\mathrm{GeV}$. The quasi-real photons at HERA are actually not monoenergetic, but have a distribution in energy given approximately by the Weizsäcker-Williams approximation. However, in general we have found little energy dependence in the energy range

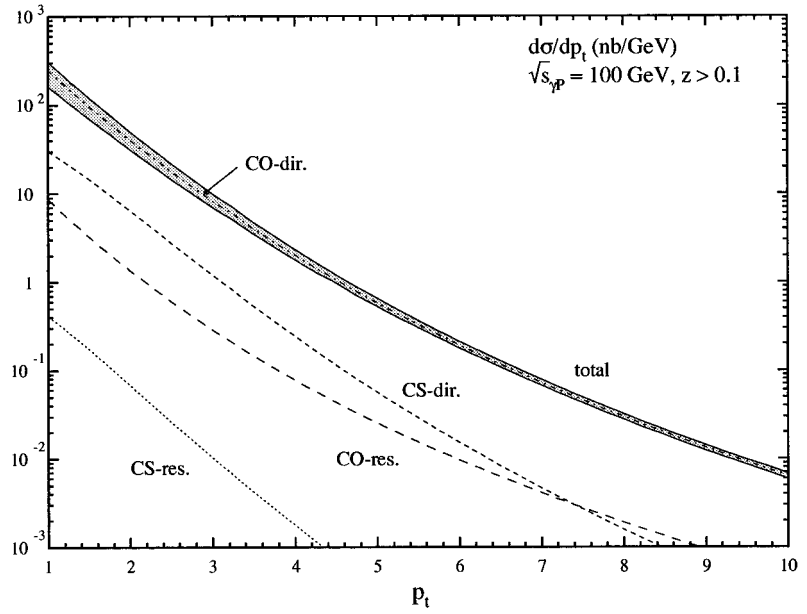

FIG. 2. Color-singlet (CS) and color-octet (CO) contributions due to direct and resolved photons to the J/ψ transverse momentum distribution $d\sigma/dp_t$ at the photon-proton center-of-mass energy $\sqrt{s_{\gamma p}}=100$ GeV; z is integrated to its upper kinematic limit. Other specifications are as in Fig. 1.

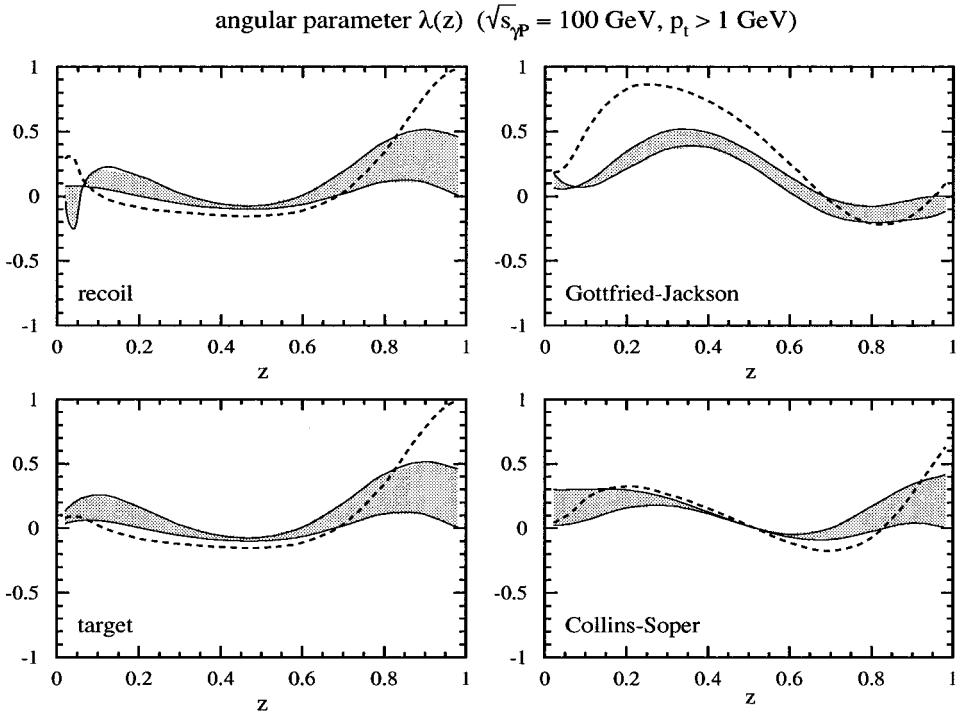

FIG. 3. Angular parameter λ of the decay angular distribution as a function of z. Direct and resolved photons are included. The dashed line is the color-singlet model prediction. The shaded area shows the NRQCD prediction bounded by the choice of parameters according to scenarios I and II. Other parameters are as in Fig. 1.

relevant to HERA (the only exception being the predictions in the recoil frame at $z \lesssim 0.3$) and thus considered a single energy.

Since the decay angular distribution parameters are normalized, the dependence on parameters that affect the absolute normalization of cross sections, such as the charm quark mass, strong coupling, the renormalization/factorization scale and parton distribution, cancels to a large extent and does not constitute a significant uncertainty.

The parameters λ, μ, ν as function of z are shown in Figs. 3–5, which include direct and resolved photon contributions. We computed the decay angular distribution parameters in four commonly used frames (recoil or s-channel helicity frame, Gottfried-Jackson frame, target frame and Collins-Soper frame) defined in Appendix A. Each plot exhibits the result from the color-singlet channel alone (dashed line) and the result after including the color-octet contributions. The two solid lines correspond to the two scenarios for the color-octet matrix elements discussed in Sec. III. Recall that the J/ψ is unpolarized, if it originates from a $c\bar{c}$ pair in a $^1S_0$ state. Thus, in scenario I the angular parameters λ, μ, ν tend to zero in regions where the color-octet processes dominate.

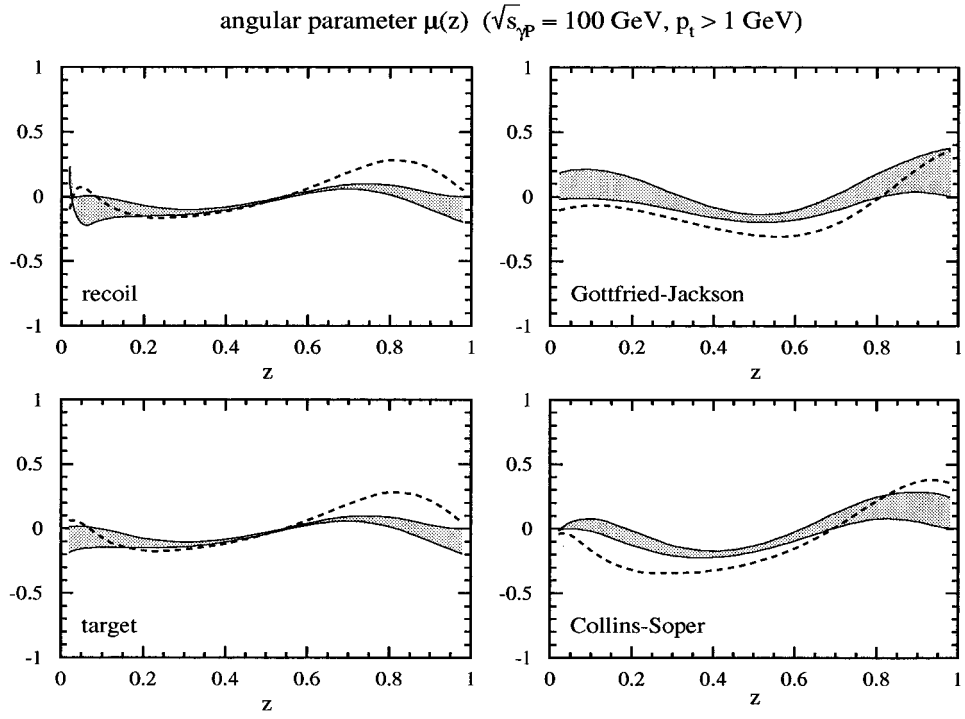

FIG. 4. Angular parameter μ of the decay angular distribution as a function of z. Direct and resolved photons are included. The dashed line is the color-singlet model prediction. The shaded area shows the NRQCD prediction bounded by the choice of parameters according to scenarios I and II. Other parameters are as in Fig. 1.

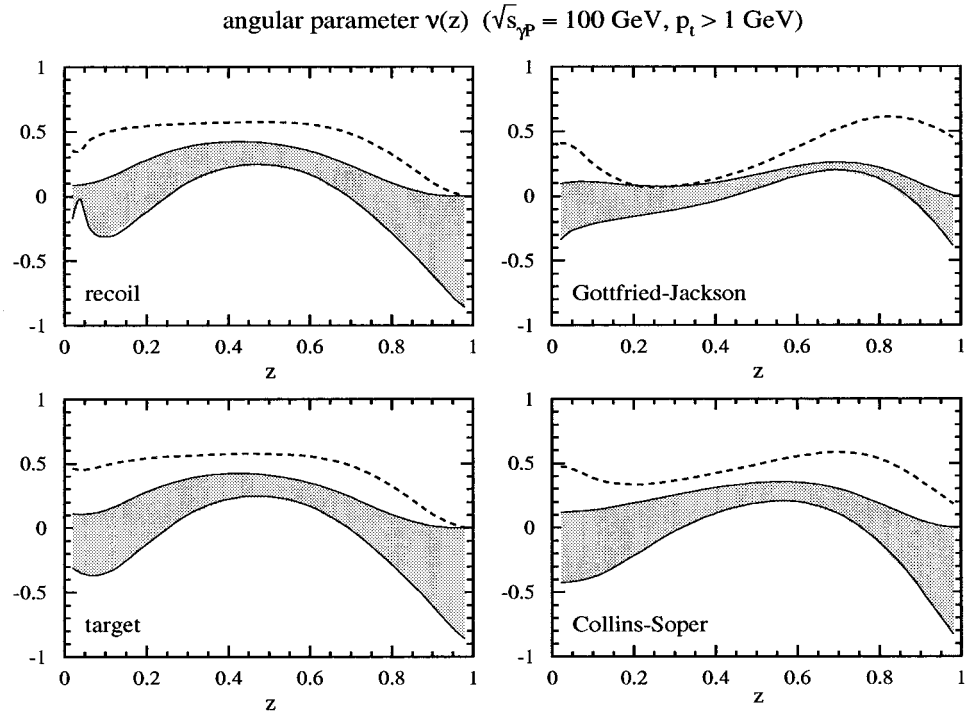

FIG. 5. Angular parameter ν of the decay angular distribution as a function of z. Direct and resolved photons are included. The dashed line is the color-singlet model prediction. The shaded area shows the NRQCD prediction bounded by the choice of parameters according to scenarios I and II. Other parameters are as in Fig. 1.

Inspecting Fig. 3, we note that in the recoil, target and Collins-Soper frames λ differs from the color-singlet prediction only in the endpoint region. The comparison looks different in the Gottfried-Jackson frame: for $z \lesssim 0.5$ the color-singlet channel yields large and positive values of λ, while the color-octet contributions yield almost unpolarized J/ψ. The azimuthal parameter μ (Fig. 4) turns out to be least interesting. We find that in all frames μ is relatively flat and close to zero, for both the color-singlet and color-octet contributions. The parameter ν, on the other hand, is very different in the color-singlet channel and after inclusion of color-octet contributions, even in the intermediate region of z, where the color-singlet channel dominates. As can be seen from Fig. 5, this difference is present in all frames and seems to make ν the most useful parameter to find out about the relative magnitude of color-singlet and color-octet contributions experimentally. To determine ν one could measure the decay angular distribution integrated over the polar angle [cf. (16)],

$$\frac{d\sigma}{d\phi\, dy} \propto 1 + \frac{\lambda(y)}{3} + \frac{\nu(y)}{3} \cos 2\phi, \tag{18}$$

or project on ν as follows:

$$\nu(y) = \frac{8}{3} \cdot \frac{\int d\Omega\, \cos(2\phi)\, \dfrac{d\sigma}{d\Omega\, dy}}{\int d\Omega \left(1 - \dfrac{5}{3}\cos^2\theta\right) \dfrac{d\sigma}{d\Omega\, dy}}. \tag{19}$$

A distinctive signature of color-octet contributions in the large-z region could be of interest in connection with the difficulties in predicting the total cross section in the endpoint region. However, the endpoint region in Figs. 3–5 is not without problems either. The higher-order terms in the velocity expansion that need to be resummed close to the endpoint lead to a convolution of the z distribution with certain nonperturbative shape functions. These shape functions depend on the production channel ($^3S_1^{(1)}$, $^1S_0^{(8)}$, and $^3P_J^{(8)}$) but they are the same for all density matrix elements in every given production channel. As a consequence, while the energy distribution itself depends on these shape functions, the *moments* in z of the normalized angular parameters depend only on the difference of the shape functions in the various production channels. Since we do expect such differences, especially between the color-singlet and the color-octet channels (due to the different properties with respect to soft gluon radiation), and since we are interested in the z distribution rather than its moments, the predictions for the angular parameters in the endpoint region still depend on these shape functions. However, this dependence is strong only if the angular parameter varies strongly in the endpoint region and disappears entirely if its distribution is flat.

In Figs. 6–8 we present the same analysis for the p_t distribution. We note that z is integrated up to its kinematic maximum. As a consequence the cross section is color-octet dominated and the color-singlet contribution plays no role for the solid curves. Since the color-octet cross section is dominated by the large-z region, the solid curves are entirely determined by the polarization yield of octet mechanisms at large z. Contrary to the situation of hadroproduction at the Tevatron, where one expects large transverse polarization due to gluon fragmentation into color-octet $c\bar{c}$ pairs [24], the photoproduction cross section tends to be unpolarized in the p_t region considered here. Therefore, the p_t distributions do not discriminate between the theoretical prediction based on NRQCD and that of the color evaporation model, which always predicts unpolarized J/ψ.

On the other hand, the transverse momentum distribution seems to prove very useful to determine the relative magnitude of color-singlet and color-octet contributions: If the

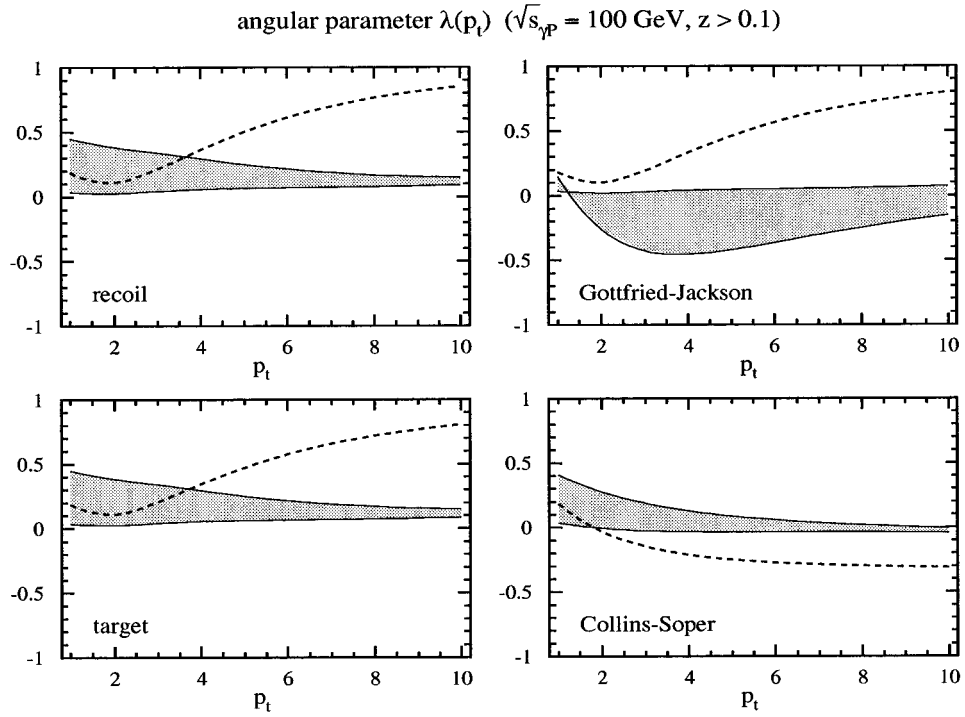

FIG. 6. Angular parameter λ of the decay angular distribution as a function of p_t. Direct and resolved photons are included. The dashed line is the color-singlet model prediction. The shaded area shows the NRQCD prediction bounded by the choice of parameters according to scenarios I and II. Other parameters are as in Fig. 1.

cross section is dominated by the color-singlet channel, large and positive values of the polar angular parameter λ (Fig. 6) are expected for $p_t \gtrsim 5$ GeV in the recoil, Gottfried-Jackson and target frames. A similar distinctive difference between color-singlet and color-octet channels is visible in the azimuthal parameter ν as defined in the Collins-Soper frame; see Fig. 8.

The unique transverse polarization signature of gluon fragmentation could possibly be made visible in the resolved photon contribution. If the direct photon contribution is reduced by a cut on the high-z region, the resolved cross section is dominated by $g \to c\bar{c}[^3S_1^{(8)}]$ at large transverse momentum [16]. As for hadroproduction [29,26], we expect that $p_t \gtrsim (5-10)$ GeV is necessary to suppress sufficiently the other color-octet channels.

V. CONCLUSION

We presented an analysis of the full polar and azimuthal decay angular distributions of inelastically photoproduced J/ψ based on the NRQCD factorization approach to quarkonium production. The primary motivation of this study is to

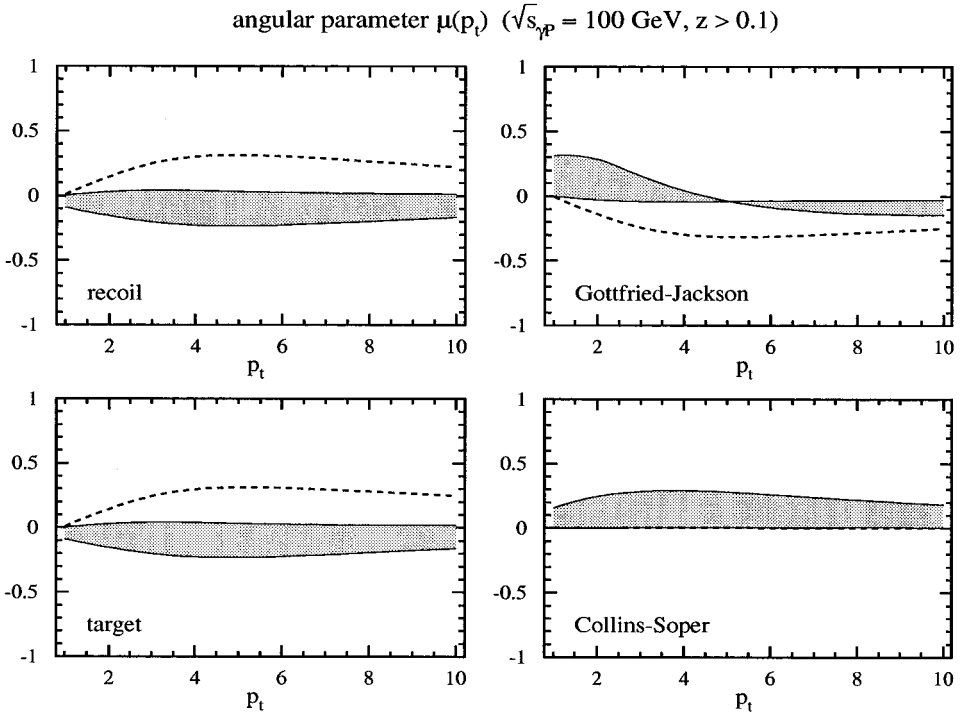

FIG. 7. Angular parameter μ of the decay angular distribution as a function of p_t. Direct and resolved photons are included. The dashed line is the color-singlet model prediction. The shaded area shows the NRQCD prediction bounded by the choice of parameters according to scenarios I and II. Other parameters are as in Fig. 1.

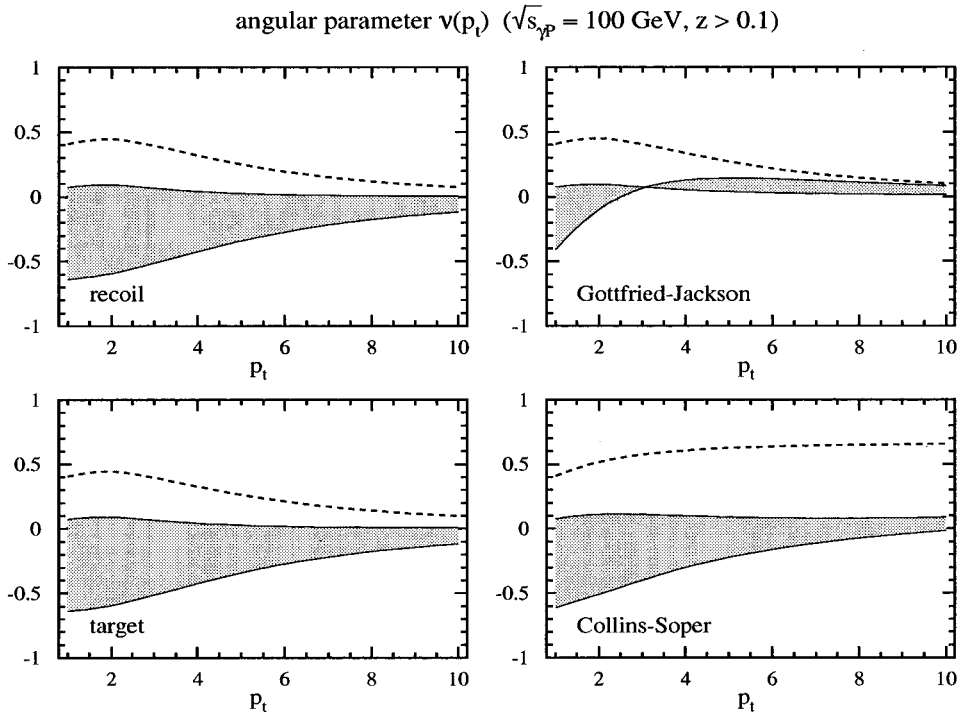

FIG. 8. Angular parameter ν of the decay angular distribution as a function of p_t. Direct and resolved photons are included. The dashed line is the color-singlet model prediction. The shaded area shows the NRQCD prediction bounded by the choice of parameters according to scenarios I and II. Other parameters are as in Fig. 1.

find observables in addition to angular-integrated differential cross sections, which are sensitive to different theories and models of quarkonium production. A particular emphasis is on clarifying the role of color-octet contributions suggested by NRQCD and other quarkonium production processes in comparison with the color-singlet model, which can be considered as a successful description of photoproduction as far as present, limited, data on energy and transverse momentum distributions is concerned.

Assuming NRQCD long-distance parameters as constrained by other J/ψ production processes such as in hadroproduction and B decay, we have found that the azimuthal decay angle distribution as a function of z or p_t would be extremely useful for discriminating between the color-singlet model and NRQCD and, to a lesser extent, the colour evaporation model. We also noted that transverse-momentum distributions integrated over all energy fraction z are color-octet dominated and could give meaningful constraints on color-octet matrix elements from the angular integrated rate as well as the decay angle dependence.

While this paper was being written, Fleming and Mehen [44] presented a study of leptoproduction of J/ψ in NRQCD, which is complementary to our photoproduction analysis. Contrary to photoproduction, the leading-twist partonic diagrams at $O(\alpha\alpha_s)$ can be sensibly compared with a total leptoproduction cross section for large enough photon virtuality Q^2. Fleming and Mehen computed the polar angle distribution due to these leading-order mechanisms and also find interesting tests of NRQCD.

ACKNOWLEDGMENTS

We would like to thank J. G. Körner for useful discussions. M.B. wishes to thank John Collins for supplying a FORTRAN integration routine.

APPENDIX A: POLARIZATION FRAMES

We collect here the covariant expressions for polarization vectors in the four commonly used frames, following [45]. [Note that the metric $g_{\mu\nu}=\mathrm{diag}(-1,1,1,1)$ is used there.]

Let p_γ be the photon momentum, p_p the photon momentum, P the momentum of quarkonium ψ and $s=(p_\gamma+p_p)^2$. We define the auxiliary vectors

$$A=p_\gamma+p_p, \quad \widetilde{A}^\mu=A^\mu-\frac{A\cdot P P^\mu}{M^2}, \tag{A1}$$

$$B=p_\gamma-p_p, \quad \widetilde{B}^\mu=B^\mu-\frac{B\cdot P P^\mu}{M^2}, \tag{A2}$$

where M is the ψ mass. (We take $M=2m_c$ in the analysis. The proton mass will be neglected in the following.) Note that $\widetilde{A},\widetilde{B}$ are three-vectors in the ψ-rest frame. We then define a coordinate system as follows.

(1) Choose $Z^\mu=\alpha_z\widetilde{A}^\mu+\beta_z\widetilde{B}^\mu$, with $Z^2=-1$.

(2) Define $X^\mu=\alpha_x\widetilde{A}^\mu+\beta_x\widetilde{B}^\mu$ in the plane spanned by $\widetilde{A},\widetilde{B}$, orthogonal to Z and normalized: $X\cdot Z=0$, $X^2=-1$.

(3) Take Y to complete a right-handed coordinate system in the ψ-rest frame,

$$Y^\mu=\frac{1}{M}\,\epsilon^{\mu\alpha\beta\gamma}P_\alpha X_\beta Z_\gamma \tag{A3}$$

($\epsilon^{0123}=1$). The sign ambiguity in α_x,β_x left in the second step is fixed by requiring $\vec{Y}$ to point in the direction of $\vec{p}_\gamma\times(-\vec{p}_p)$ in the ψ-rest frame, which requires $\alpha_z\beta_x-\alpha_x\beta_z>0$.

The four commonly used polarization frames are then specified by the choice of Z. In the *recoil* (or s-channel helicity) frame, the Z axis is defined as the direction of the ψ

three-momentum in the hadronic center-of-mass frame, that is $\vec{Z}=-\vec{A}/|\vec{A}|$ in the ψ-rest frame. In the *Gottfried-Jackson* frame $\vec{Z}=\vec{p}_\gamma/|\vec{p}_\gamma|$ and in the *target* frame $\vec{Z}=-\vec{p}_p/|\vec{p}_p|$. In the *Collins-Soper* frame the Z axis bisects the angle between $\vec{p}_\gamma$ and $(-\vec{p}_p)$, i.e., $\vec{Z}\propto\vec{p}_\gamma|/|\vec{p}_\gamma|+(-\vec{p}_p)/|\vec{p}_p|$. (All three-vectors refer to the ψ-rest frame.) We then find the covariant expressions for the coordinate axes from the following expressions for $\alpha_{z,x}, \beta_{z,x}$.

Recoil frame:

$$\alpha_z=-\frac{M}{\sqrt{(A\cdot P)^2-M^2s}},\quad \beta_z=0, \tag{A4}$$

$$\alpha_x=\frac{A\cdot PB\cdot P}{\sqrt{s((A\cdot P)^2-M^2s)((A\cdot P)^2-(B\cdot P)^2-M^2s)}}, \tag{A5}$$

$$\beta_x=-\frac{\sqrt{(A\cdot P)^2-M^2s}}{\sqrt{s((A\cdot P)^2-(B\cdot P)^2-M^2s)}}. \tag{A6}$$

Gottfried-Jackson frame:

$$\alpha_z=\beta_z=\frac{M}{A\cdot P+B\cdot P}, \tag{A7}$$

$$\alpha_x=-\frac{(B\cdot P)^2+A\cdot PB\cdot P+M^2s}{(A\cdot P+B\cdot P)\sqrt{s((A\cdot P)^2-(B\cdot P)^2-M^2s)}}, \tag{A8}$$

$$\beta_x=\frac{(A\cdot P)^2+A\cdot PB\cdot P-M^2s}{(A\cdot P+B\cdot P)\sqrt{s((A\cdot P)^2-(B\cdot P)^2-M^2s)}}. \tag{A9}$$

Target frame:

$$\alpha_z=-\beta_z=-\frac{M}{A\cdot P-B\cdot P}, \tag{A10}$$

$$\alpha_x=-\frac{(B\cdot P)^2-A\cdot PB\cdot P+M^2s}{(A\cdot P-B\cdot P)\sqrt{s((A\cdot P)^2-(B\cdot P)^2-M^2s)}}, \tag{A11}$$

$$\beta_x=-\frac{(A\cdot P)^2-A\cdot PB\cdot P-M^2s}{(A\cdot P-B\cdot P)\sqrt{s((A\cdot P)^2-(B\cdot P)^2-M^2s)}}. \tag{A12}$$

Collins-Soper frame:

$$\alpha_z=-\frac{B\cdot P}{\sqrt{s((A\cdot P)^2-(B\cdot P)^2)}},\quad \beta_z=\frac{A\cdot P}{\sqrt{s((A\cdot P)^2-(B\cdot P)^2)}}, \tag{A13}$$

$$\alpha_x=-\frac{MA\cdot P}{\sqrt{((A\cdot P)^2-(B\cdot P)^2)((A\cdot P)^2-(B\cdot P)^2-M^2s)}}, \tag{A14}$$

$$\beta_x=\frac{MB\cdot P}{\sqrt{((A\cdot P)^2-(B\cdot P)^2)((A\cdot P)^2-(B\cdot P)^2-M^2s)}}. \tag{A15}$$

We note that $A\cdot P+B\cdot P=(P_t^2+M^2)/z$ and $A\cdot P-B\cdot P=sz$. Finally, the polarization vectors are given by

$$\epsilon^\mu(\lambda=0)=Z^\mu, \quad \epsilon^\mu(\lambda=\pm 1)=\frac{1}{\sqrt{2}}\,(\mp X^\mu - iY^\mu). \tag{A16}$$

APPENDIX B: DENSITY MATRICES

The density matrices for all processes considered in the paper are given in this Appendix. The results given for the resolved photon process apply equally to J/ψ production in hadron-hadron collisions and have been used in [26]. The functions of F, a, b, c, d below are related to A, B, C, D of (15) as $A=Fa$, etc., and we suppressed all sub and superscripts. For the partonic process $1+2\to 3+4$, the Mandelstam invariants are $\hat{s}=(p_1+p_2)^2$, $\hat{t}=(p_3-p_1)^2$, $\hat{u}=(p_3-p_2)^2$.

1. Direct-photon processes

$\gamma+g\to c\bar{c}[^3S_1^{(1)}]+g$:

$$F=\frac{16M(4\pi)^3\alpha\alpha_s^2e_c^2\langle\mathcal{O}_1^{J/\psi}(^3S_1)\rangle}{27[(\hat{s}-M^2)(\hat{t}-M^2)(\hat{u}-M^2)]^2}, \tag{B1}$$

$$a=-(\hat{s}^2+\hat{s}\hat{t}+\hat{t}^2)^2+M^2(2\hat{s}^2+\hat{s}\hat{t}+2\hat{t}^2)(\hat{s}+\hat{t})-M^4(\hat{s}^2+\hat{s}\hat{t}+\hat{t}^2), \tag{B2}$$

$$b=-2(\hat{s}^2+\hat{t}^2), \tag{B3}$$

$$c=-2(\hat{s}^2+\hat{u}^2), \tag{B4}$$

$$d=-2\hat{s}^2. \tag{B5}$$

$\gamma+g\to c\bar{c}[^3S_1^{(8)}]+g$: a,b,c,d are the same as (B2)–(B5), F is multiplied by

$$\frac{15}{8}\cdot\frac{\langle\mathcal{O}_8^{J/\psi}(^3S_1)\rangle}{\langle\mathcal{O}_1^{J/\psi}(^3S_1)\rangle}. \tag{B6}$$

$\gamma+g\to c\bar{c}[^1S_0^{(8)}]+g$:

$$F_a=-\frac{2(4\pi)^3\alpha\alpha_s^2e_c^2\langle\mathcal{O}_8^{J/\psi}(^1S_0)\rangle}{M\hat{t}[(\hat{s}-M^2)(\hat{t}-M^2)(\hat{u}-M^2)]^2}\,\hat{s}\hat{u}\{[\hat{u}^2-M^2(\hat{u}-M^2)]^2-2\hat{s}\hat{t}(\hat{u}-M^2)^2+\hat{s}^2\hat{t}^2\}, \tag{B7}$$

$$b=c=d=0. \tag{B8}$$

$\gamma+g\to c\bar{c}[^3P_J^{(8)}]+g$:

$$F=-\frac{24(4\pi)^3\alpha\alpha_s^2e_c^2\langle\mathcal{O}_8^{J/\psi}(^3P_0)\rangle}{\hat{t}^2[M(\hat{s}-M^2)(\hat{t}-M^2)(\hat{u}-M^2)]^3}, \tag{B9}$$

$$\begin{aligned}a=&\hat{s}^2\hat{t}^2(\hat{s}+\hat{t})^2(\hat{s}^2+\hat{s}\hat{t}+\hat{t}^2)^2-M^2\hat{s}\hat{t}(\hat{s}^7+8\hat{s}^6\hat{t}+16\hat{s}^5\hat{t}^2+16\hat{s}^4\hat{t}^3+8\hat{s}^3\hat{t}^4-3\hat{s}\hat{t}^6-2\hat{t}^7)\\&+M^4\hat{t}(4\hat{s}^7+28\hat{s}^6\hat{t}+48\hat{s}^5\hat{t}^2+41\hat{s}^4\hat{t}^3+18\hat{s}^3\hat{t}^4-4\hat{s}\hat{t}^6+\hat{t}^7)-M^6\hat{t}(12\hat{s}^6+64\hat{s}^5\hat{t}+99\hat{s}^4\hat{t}^2+80\hat{s}^3\hat{t}^3+33\hat{s}^2\hat{t}^4+3\hat{s}\hat{t}^5+3\hat{t}^6)\\&+M^8\hat{t}(22\hat{s}^5+88\hat{s}^4\hat{t}+114\hat{s}^3\hat{t}^2+67\hat{s}^2\hat{t}^3+14\hat{s}\hat{t}^4+3\hat{t}^5)-M^{10}\hat{t}(22\hat{s}^4+68\hat{s}^3\hat{t}+61\hat{s}^2\hat{t}^2+16\hat{s}\hat{t}^3+\hat{t}^4)\\&+2M^{12}\hat{s}\hat{t}(6\hat{s}^2+13\hat{s}\hat{t}+5\hat{t}^2)-3M^{14}\hat{s}\hat{t}(\hat{s}+\hat{t}),\end{aligned} \tag{B10}$$

$$\begin{aligned}b=&-2(\hat{s}+\hat{t})^4(2\hat{s}^4+\hat{s}^2\hat{t}^2+2\hat{t}^4)+2M^2(6\hat{s}^7+19\hat{s}^6\hat{t}+21\hat{s}^5\hat{t}^2+17\hat{s}^4\hat{t}^3+21\hat{s}^3\hat{t}^4+28\hat{s}^2\hat{t}^5+22\hat{s}\hat{t}^6+6\hat{t}^7)\\&-2M^4(6\hat{s}^6+9\hat{s}^5\hat{t}-15\hat{s}^4\hat{t}^2-24\hat{s}^3\hat{t}^3-4\hat{s}^2\hat{t}^4+15\hat{s}\hat{t}^5+5\hat{t}^6)+2M^6(2\hat{s}^5-10\hat{s}^4\hat{t}-45\hat{s}^3\hat{t}^2-37\hat{s}^2\hat{t}^3-3\hat{s}\hat{t}^4+\hat{t}^5)\\&+8M^8\hat{s}\hat{t}(3\hat{s}^2+7\hat{s}\hat{t}+2\hat{t}^2)-8M^{10}\hat{s}\hat{t}(\hat{s}+\hat{t}),\end{aligned} \tag{B11}$$

$$\begin{aligned}c=&2\hat{t}^2(2\hat{s}^6+6\hat{s}^5\hat{t}+5\hat{s}^4\hat{t}^2-7\hat{s}^2\hat{t}^4-6\hat{s}\hat{t}^5-2\hat{t}^6)+2M^2\hat{t}^2(-6\hat{s}^5-9\hat{s}^4\hat{t}+2\hat{s}^3\hat{t}^2+21\hat{s}^2\hat{t}^3+22\hat{s}\hat{t}^4+8\hat{t}^5)\\&-2M^4(2\hat{s}^6+6\hat{s}^5\hat{t}-11\hat{s}^4\hat{t}^2-20\hat{s}^3\hat{t}^3+7\hat{s}^2\hat{t}^4+27\hat{s}\hat{t}^5+11\hat{t}^6)+2M^6(6\hat{s}^5+15\hat{s}^4\hat{t}-12\hat{s}^3\hat{t}^2-19\hat{s}^2\hat{t}^3+8\hat{s}\hat{t}^4+4\hat{t}^5)\\&-4M^8(3\hat{s}^4+6\hat{s}^3\hat{t}-4\hat{s}^2\hat{t}^2-3\hat{s}\hat{t}^3-2\hat{t}^4)+4M^{10}(\hat{s}^3+2\hat{s}^2\hat{t}-\hat{s}\hat{t}^2-2\hat{t}^3)-2M^{12}\hat{t}(\hat{s}-\hat{t}),\end{aligned} \tag{B12}$$

$$d=2\hat{t}^2(\hat{s}^6+2\hat{s}^5\hat{t}-6\hat{s}^3\hat{t}^3-10\hat{s}^2\hat{t}^4-7\hat{s}\hat{t}^5-2\hat{t}^6)-M^2(4\hat{s}^7+14\hat{s}^6\hat{t}+30\hat{s}^5\hat{t}^2+29\hat{s}^4\hat{t}^3+4\hat{s}^3\hat{t}^4-33\hat{s}^2\hat{t}^5-38\hat{s}\hat{t}^6-14\hat{t}^7)$$

$$+2M^4(6\hat{s}^6+21\hat{s}^5\hat{t}+43\hat{s}^4\hat{t}^2+43\hat{s}^3\hat{t}^3+13\hat{s}^2\hat{t}^4-15\hat{s}\hat{t}^5-9\hat{t}^6)-M^6(12\hat{s}^5+45\hat{s}^4\hat{t}+92\hat{s}^3\hat{t}^2+78\hat{s}^2\hat{t}^3+6\hat{s}\hat{t}^4-9\hat{t}^5)$$
$$+2M^8\hat{s}(2\hat{s}^3+11\hat{s}^2\hat{t}+22\hat{s}\hat{t}^2+9\hat{t}^3)-M^{10}\hat{t}(5\hat{s}^2+6\hat{s}\hat{t}+\hat{t}^2). \tag{B13}$$

$\gamma+q\to c\bar{c}[^3S_1^{(8)}]+g$:

$$F=\frac{(4\pi)^3\alpha\alpha_s^2e_q^2\langle\mathcal{O}_8^{J/\psi}(^3S_1)\rangle}{9M^3\hat{s}\hat{u}}, \tag{B14}$$

$$a=\hat{s}^2+\hat{u}^2+2M^2\hat{t}, \tag{B15}$$

$$b=4, \tag{B16}$$

$$c=8, \tag{B17}$$

$$d=4, \tag{B18}$$

where e_q is the electric charge of the light quark q.

$\gamma+q\to c\bar{c}[^1S_0^{(8)}]$

$$Fa=\frac{4(4\pi)^3\alpha\alpha_s^2e_c^2\langle\mathcal{O}_8^{J/\psi}(^1S_0)\rangle}{9M\hat{t}(\hat{t}-M^2)^2}\{\hat{s}^2+\hat{u}^2\}, \tag{B19}$$

$$b=c=d=0. \tag{B20}$$

$\gamma+q\to c\bar{c}[^3P_J^{(8)}]+q$:

$$F=\frac{16(4\pi)^3\alpha\alpha_s^2e_c^2\langle\mathcal{O}_8^{J/\psi}(^3P_0)\rangle}{3M^3\hat{t}^2(\hat{t}-M^2)^3}, \tag{B21}$$

$$a=\hat{t}(\hat{t}-M^2)(\hat{s}^2+\hat{u}^2+2M^2\hat{t}+2M^4), \tag{B22}$$

$$b=-8(\hat{s}^2+\hat{s}\hat{t}+M^2\hat{t}), \tag{B23}$$

$$c=8(\hat{t}^2-M^4), \tag{B24}$$

$$d=4(\hat{t}^2-2M^2\hat{s}-M^2\hat{t}). \tag{B25}$$

2. Resolved-photon processes

$g+g\to c\bar{c}[^3S_1^{(1)}]+g$: a,b,c,d are the same as (B2)–(B5), F is multiplied by

$$\frac{5}{96}\cdot\frac{\alpha_s}{\alpha e_c^2}. \tag{B26}$$

$g+g\to c\bar{c}[^3S_1^{(8)}]+g$:

$$F=\frac{(4\pi\alpha_s)^3\langle\mathcal{O}_8^{J/\psi}(^3S_1)\rangle}{144M^3[(\hat{s}-M^2)(\hat{t}-M^2)(\hat{u}-M^2)]^2}\{27(\hat{s}\hat{t}+\hat{s}\hat{u}+\hat{t}\hat{u})-19M^4\}, \tag{B27}$$

$$a=(\hat{s}^2+\hat{s}\hat{t}+\hat{t}^2)^2-M^2(2\hat{s}^2+\hat{s}\hat{t}+2\hat{t}^2)(\hat{s}+\hat{t})+M^4(\hat{s}^2+\hat{s}\hat{t}+\hat{t}^2), \tag{B28}$$

$$b=2(\hat{s}^2+\hat{t}^2), \tag{B29}$$

$$c=2(\hat{s}^2+\hat{u}^2), \tag{B30}$$

$$d=2\hat{s}^2. \tag{B31}$$

$g+g\to c\bar{c}[^1S_0^{(8)}]+g$:

$$Fa=-\frac{5(4\pi\alpha_s)^3\langle\mathcal{O}_8^{J/\psi}(^1S_0)\rangle}{48M\hat{s}\hat{t}\hat{u}[(\hat{s}-M^2)(\hat{t}-M^2)(\hat{u}-M^2)]^2}\{\hat{s}^2(\hat{s}-M^2)^2+\hat{s}\hat{t}\hat{u}(M^2-2\hat{s})+\hat{t}^2\hat{u}^2\}\{(\hat{s}^2-M^2\hat{s}+M^4)^2-\hat{t}\hat{u}(2\hat{t}^2+3\hat{t}\hat{u}+2\hat{u}^2)\}, \tag{B32}$$

$$b=c=d=0. \tag{B33}$$

$g+g\to c\bar{c}[^3P_J^{(8)}]+g$:

$$F=\frac{5(4\pi\alpha_s)^3\langle\mathcal{O}_8^{J/\psi}(^3P_0)\rangle}{4\hat{s}^2\hat{t}^2\hat{u}^2[M(\hat{s}-M^2)(\hat{t}-M^2)(\hat{u}-M^2)]^3}, \tag{B34}$$

$$\begin{aligned}a=&\hat{s}\hat{t}\hat{u}\{\hat{s}^{10}\hat{t}+5\hat{s}^9\hat{t}^2+14\hat{s}^8\hat{t}^3+26\hat{s}^7\hat{t}^4+35\hat{s}^6\hat{t}^5+35\hat{s}^5\hat{t}^6+26\hat{s}^4\hat{t}^7+14\hat{s}^3\hat{t}^8+5\hat{s}^2\hat{t}^9+\hat{s}\hat{t}^{10}\\&-M^2(\hat{s}^{10}+10\hat{s}^9\hat{t}+26\hat{s}^8\hat{t}^2+40\hat{s}^7\hat{t}^3+45\hat{s}^6\hat{t}^4+44\hat{s}^5\hat{t}^5+45\hat{s}^4\hat{t}^6+40\hat{s}^3\hat{t}^7+26\hat{s}^2\hat{t}^8+10\hat{s}\hat{t}^9+\hat{t}^{10})\\&+M^4(5\hat{s}^9+40\hat{s}^8\hat{t}+84\hat{s}^7\hat{t}^2+106\hat{s}^6\hat{t}^3+103\hat{s}^5\hat{t}^4+103\hat{s}^4\hat{t}^5+106\hat{s}^3\hat{t}^6+84\hat{s}^2\hat{t}^7+40\hat{s}\hat{t}^8+5\hat{t}^9)\\&-M^6(16\hat{s}^8+104\hat{s}^7\hat{t}+215\hat{s}^6\hat{t}^2+291\hat{s}^5\hat{t}^3+316\hat{s}^4\hat{t}^4+291\hat{s}^3\hat{t}^5+215\hat{s}^2\hat{t}^6+104\hat{s}\hat{t}^7+16\hat{t}^8)+M^8(34\hat{s}^7+179\hat{s}^6\hat{t}+356\hat{s}^5\hat{t}^2\\&+473\hat{s}^4\hat{t}^3+473\hat{s}^3\hat{t}^4+356\hat{s}^2\hat{t}^5+179\hat{s}\hat{t}^6+34\hat{t}^7)-M^{10}(44\hat{s}^6+193\hat{s}^5\hat{t}+346\hat{s}^4\hat{t}^2+410\hat{s}^3\hat{t}^3+346\hat{s}^2\hat{t}^4+193\hat{s}\hat{t}^5+44\hat{t}^6)\\&+M^{12}(34\hat{s}^5+124\hat{s}^4\hat{t}+188\hat{s}^3\hat{t}^2+188\hat{s}^2\hat{t}^3+124\hat{s}\hat{t}^4+34\hat{t}^5)\\&-M^{14}(15\hat{s}^4+43\hat{s}^3\hat{t}+52\hat{s}^2\hat{t}^2+43\hat{s}\hat{t}^3+15\hat{t}^4)+M^{16}(3\hat{s}^3+6\hat{s}^2\hat{t}+6\hat{s}\hat{t}^2+3\hat{t}^3)\},\end{aligned} \tag{B35}$$

$$\begin{aligned}b=&4\hat{s}^{12}+24\hat{s}^{11}\hat{t}+68\hat{s}^{10}\hat{t}^2+124\hat{s}^9\hat{t}^3+164\hat{s}^8\hat{t}^4+176\hat{s}^7\hat{t}^5+176\hat{s}^6\hat{t}^6+176\hat{s}^5\hat{t}^7+164\hat{s}^4\hat{t}^8+124\hat{s}^3\hat{t}^9+68\hat{s}^2\hat{t}^{10}+24\hat{s}\hat{t}^{11}+4\hat{t}^{12}\\&-M^2(20\hat{s}^{11}+104\hat{s}^{10}\hat{t}+250\hat{s}^9\hat{t}^2+397\hat{s}^8\hat{t}^3+481\hat{s}^7\hat{t}^4+500\hat{s}^6\hat{t}^5+500\hat{s}^5\hat{t}^6+481\hat{s}^4\hat{t}^7+397\hat{s}^3\hat{t}^8+250\hat{s}^2\hat{t}^9+104\hat{s}\hat{t}^{10}+20\hat{t}^{11})\\&+M^4(40\hat{s}^{10}+166\hat{s}^9\hat{t}+278\hat{s}^8\hat{t}^2+285\hat{s}^7\hat{t}^3+206\hat{s}^6\hat{t}^4+146\hat{s}^5\hat{t}^5+206\hat{s}^4\hat{t}^6+285\hat{s}^3\hat{t}^7+278\hat{s}^2\hat{t}^8+166\hat{s}\hat{t}^9+40\hat{t}^{10})\\&+M^6(-40\hat{s}^9-97\hat{s}^8\hat{t}+53\hat{s}^7\hat{t}^2+373\hat{s}^6\hat{t}^3+647\hat{s}^5\hat{t}^4+647\hat{s}^4\hat{t}^5+373\hat{s}^3\hat{t}^6+53\hat{s}^2\hat{t}^7-97\hat{s}\hat{t}^8-40\hat{t}^9)\\&+M^8(20\hat{s}^8-33\hat{s}^7\hat{t}-368\hat{s}^6\hat{t}^2-751\hat{s}^5\hat{t}^3-920\hat{s}^4\hat{t}^4-751\hat{s}^3\hat{t}^5-368\hat{s}^2\hat{t}^6-33\hat{s}\hat{t}^7+20\hat{t}^8)\\&+M^{10}(-4\hat{s}^7+77\hat{s}^6\hat{t}+323\hat{s}^5\hat{t}^2+492\hat{s}^4\hat{t}^3+492\hat{s}^3\hat{t}^4+323\hat{s}^2\hat{t}^5+77\hat{s}\hat{t}^6-4\hat{t}^7)-M^{12}(41\hat{s}^5\hat{t}+120\hat{s}^4\hat{t}^2+142\hat{s}^3\hat{t}^3+120\hat{s}^2\hat{t}^4\\&+41\hat{s}\hat{t}^5)+M^{14}(8\hat{s}^4\hat{t}+16\hat{s}^3\hat{t}^2+16\hat{s}^2\hat{t}^3+8\hat{s}\hat{t}^4),\end{aligned} \tag{B36}$$

$$\begin{aligned}c=&-4\hat{s}^{10}\hat{t}^2-20\hat{s}^9\hat{t}^3-40\hat{s}^8\hat{t}^4-40\hat{s}^7\hat{t}^5+8\hat{s}^6\hat{t}^6+80\hat{s}^5\hat{t}^7+128\hat{s}^4\hat{t}^8+116\hat{s}^3\hat{t}^9+68\hat{s}^2\hat{t}^{10}+24\hat{s}\hat{t}^{11}+4\hat{t}^{12}\\&+M^2(20\hat{s}^9\hat{t}^2+56\hat{s}^8\hat{t}^3+24\hat{s}^7\hat{t}^4-147\hat{s}^6\hat{t}^5-409\hat{s}^5\hat{t}^6-599\hat{s}^4\hat{t}^7-571\hat{s}^3\hat{t}^8-370\hat{s}^2\hat{t}^9-148\hat{s}\hat{t}^{10}-28\hat{t}^{11})\\&+M^4(4\hat{s}^{10}+20\hat{s}^9\hat{t}-16\hat{s}^8\hat{t}^2-48\hat{s}^7\hat{t}^3+150\hat{s}^6\hat{t}^4+611\hat{s}^5\hat{t}^5+1060\hat{s}^4\hat{t}^6+1155\hat{s}^3\hat{t}^7+854\hat{s}^2\hat{t}^8+394\hat{s}\hat{t}^9+84\hat{t}^{10})\\&-M^6(20\hat{s}^9+88\hat{s}^8\hat{t}+48\hat{s}^7\hat{t}^2+12\hat{s}^6\hat{t}^3+318\hat{s}^5\hat{t}^4+863\hat{s}^4\hat{t}^5+1195\hat{s}^3\hat{t}^6+1061\hat{s}^2\hat{t}^7+583\hat{s}\hat{t}^8+140\hat{t}^9)\\&+M^8(40\hat{s}^8+152\hat{s}^7\hat{t}+94\hat{s}^6\hat{t}^2+38\hat{s}^5\hat{t}^3+290\hat{s}^4\hat{t}^4+631\hat{s}^3\hat{t}^5+738\hat{s}^2\hat{t}^6+513\hat{s}\hat{t}^7+140\hat{t}^8)\\&-M^{10}(40\hat{s}^7+129\hat{s}^6\hat{t}+53\hat{s}^5\hat{t}^2+7\hat{s}^4\hat{t}^3+129\hat{s}^3\hat{t}^4+264\hat{s}^2\hat{t}^5+266\hat{s}\hat{t}^6+84\hat{t}^7)+M^{12}(20\hat{s}^6+55\hat{s}^5\hat{t}+2\hat{s}^4\hat{t}^2\\&-15\hat{s}^3\hat{t}^3+30\hat{s}^2\hat{t}^4+76\hat{s}\hat{t}^5+28\hat{t}^6)\\&+M^{14}(-4\hat{s}^5-11\hat{s}^4\hat{t}+7\hat{s}^3\hat{t}^2+7\hat{s}^2\hat{t}^3-11\hat{s}\hat{t}^4-4\hat{t}^5)+M^{16}(\hat{s}^3\hat{t}-2\hat{s}^2\hat{t}^2+\hat{s}\hat{t}^3),\end{aligned} \tag{B37}$$

$$\begin{aligned}d=&-2\hat{s}^{10}\hat{t}^2-6\hat{s}^9\hat{t}^3-2\hat{s}^8\hat{t}^4+28\hat{s}^7\hat{t}^5+88\hat{s}^6\hat{t}^6+148\hat{s}^5\hat{t}^7+166\hat{s}^4\hat{t}^8+130\hat{s}^3\hat{t}^9+70\hat{s}^2\hat{t}^{10}+24\hat{s}\hat{t}^{11}+4\hat{t}^{12}\\&+M^2(4\hat{s}^{11}+22\hat{s}^{10}\hat{t}+70\hat{s}^9\hat{t}^2+115\hat{s}^8\hat{t}^3+71\hat{s}^7\hat{t}^4-119\hat{s}^6\hat{t}^5-381\hat{s}^5\hat{t}^6-552\hat{s}^4\hat{t}^7-512\hat{s}^3\hat{t}^8-320\hat{s}^2\hat{t}^9-126\hat{s}\hat{t}^{10}\\&-24\hat{t}^{11})+M^4(-20\hat{s}^{10}-104\hat{s}^9\hat{t}-296\hat{s}^8\hat{t}^2-459\hat{s}^7\hat{t}^3-352\hat{s}^6\hat{t}^4+73\hat{s}^5\hat{t}^5+558\hat{s}^4\hat{t}^6+744\hat{s}^3\hat{t}^7+574\hat{s}^2\hat{t}^8\\&+270\hat{s}\hat{t}^9+60\hat{t}^{10})+M^6(40\hat{s}^9+199\hat{s}^8\hat{t}+533\hat{s}^7\hat{t}^2+778\hat{s}^6\hat{t}^3+596\hat{s}^5\hat{t}^4+51\hat{s}^4\hat{t}^5-405\hat{s}^3\hat{t}^6-480\hat{s}^2\hat{t}^7-296\hat{s}\hat{t}^8-80\hat{t}^9)\\&+M^8(-40\hat{s}^8-197\hat{s}^7\hat{t}-506\hat{s}^6\hat{t}^2-672\hat{s}^5\hat{t}^3-460\hat{s}^4\hat{t}^4-79\hat{s}^3\hat{t}^5+138\hat{s}^2\hat{t}^6+164\hat{s}\hat{t}^7+60\hat{t}^8)\\&+M^{10}(20\hat{s}^7+107\hat{s}^6\hat{t}+267\hat{s}^5\hat{t}^2+307\hat{s}^4\hat{t}^3+185\hat{s}^3\hat{t}^4+56\hat{s}^2\hat{t}^5-30\hat{s}\hat{t}^6-24\hat{t}^7)\\&+M^{12}(-4\hat{s}^6-31\hat{s}^5\hat{t}-74\hat{s}^4\hat{t}^2-71\hat{s}^3\hat{t}^3-46\hat{s}^2\hat{t}^4-10\hat{s}\hat{t}^5+4\hat{t}^6)+M^{14}(4\hat{s}^4\hat{t}+8\hat{s}^3\hat{t}^2+8\hat{s}^2\hat{t}^3+4\hat{s}\hat{t}^4).\end{aligned} \tag{B38}$$

$g+q\to c\bar{c}[^3S_1^{(8)}]+q$:

$$F=\frac{(4\pi\alpha_s)^3\langle\mathcal{O}_8^{J/\psi}(^3S_1)\rangle}{216M^3\hat{s}\hat{u}(\hat{t}-M^2)^2}\{4(\hat{t}-M^2)^2-9\hat{s}\hat{u}\}, \tag{B39}$$

$$a=\hat{s}^2+\hat{u}^2+2M^2\hat{t}, \tag{B40}$$

$$b=4, \tag{B41}$$

$$c=8, \tag{B42}$$

$$d=4. \tag{B43}$$

$g+q\to c\bar{c}[^1S_0^{(8)}]+q$:

$$Fa=\frac{5(4\pi\alpha_s)^3\langle\mathcal{O}_8^{J/\psi}(^1S_0)\rangle}{216M\hat{t}(\hat{t}-M^2)^2}\{\hat{s}^2+\hat{u}^2\}, \tag{B44}$$

$$b=c=d=0. \tag{B45}$$

$g+q\to c\bar{c}[^3P_J^{(8)}]+q$:

$$F=\frac{5(4\pi\alpha_s)^3\langle\mathcal{O}_8^{J/\psi}(^3P_0)\rangle}{18M^3\hat{t}^2(\hat{t}-M^2)^3}, \tag{B46}$$

$$a=\hat{t}(\hat{t}-M^2)(\hat{s}^2+\hat{u}^2+2M^2\hat{t}+2M^4), \tag{B47}$$

$$b=-8(\hat{s}^2+\hat{s}\hat{t}+M^2\hat{t}), \tag{B48}$$

$$c=8(\hat{t}^2-M^4), \tag{B49}$$

$$d=4(\hat{t}^2-2M^2\hat{s}-M^2\hat{t}). \tag{B50}$$

$q+\bar{q}\to c\bar{c}[^3S_1^{(8)}]+g$:

$$F=-\frac{(4\pi\alpha_s)^3\langle\mathcal{O}_8^{J/\psi}(^3S_1)\rangle}{81M^3\hat{t}\hat{u}(\hat{s}-M^2)^2}\{4(\hat{s}-M^2)^2-9\hat{t}\hat{u}\}, \tag{B51}$$

$$a=\hat{t}^2+\hat{u}^2+2M^2\hat{s}, \tag{B52}$$

$$b=4, \tag{B53}$$

$$c=4, \tag{B54}$$

$$d=0. \tag{B55}$$

$q+\bar{q}\to c\bar{c}[^1S_0^{(8)}]+g$:

$$Fa=-\frac{5(4\pi\alpha_s)^3\langle\mathcal{O}_8^{J/\psi}(^1S_0)\rangle}{81M\hat{s}(\hat{s}-M^2)^2}\{\hat{t}^2+\hat{u}^2\}, \tag{B56}$$

$$b=c=d=0. \tag{B57}$$

$q+\bar{q}\to c\bar{c}[^3P_J^{(8)}]+g$:

$$F=\frac{20(4\pi\alpha_s)\langle\mathcal{O}_8^{J/\psi}(^3P_0)\rangle}{27M^3\hat{s}^2(\hat{s}-M^2)^3}, \tag{B58}$$

$$a=-\hat{s}(\hat{s}-M^2)(\hat{t}^2+\hat{u}^2+2M^2\hat{s}+2M^4), \tag{B59}$$

$$b=8(\hat{t}^2+\hat{s}\hat{t}+M^2\hat{s}), \tag{B60}$$

$$c = 8(\hat{t}^2 + \hat{s}\hat{t} - 2M^2\hat{t} + M^4), \tag{B61}$$

$$d = 4(\hat{s}^2 + 2\hat{s}\hat{t} + 2\hat{t}^2 + M^2\hat{s} - 2M^2\hat{t}). \tag{B62}$$

[1] E. Braaten, S. Fleming, and T. C. Yuan, Annu. Rev. Nucl. Part. Sci. **46**, 197 (1996).

[2] M. Beneke, ''Lecture at the XXIVth SLAC Summer Institute on Particle Physics, August 1996,'' CERN-TH-97-55 [hep-ph/9703429].

[3] G. T. Bodwin, E. Braaten, and G. P. Lepage, Phys. Rev. D **51**, 1125 (1995); **55**, 5853(E) (1997).

[4] H. Fritzsch, Phys. Lett. **67B**, 217 (1977); F. Halzen, *ibid.* **69B**, 105 (1977); F. Halzen and S. Matsuda, Phys. Rev. D **17**, 1344 (1978); M. Glück, J. Owens, and E. Reya, *ibid.* **17**, 2324 (1978).

[5] R. Gavai *et al.*, Int. J. Mod. Phys. A **10**, 3043 (1995); J. F. Amundson, O. J. P. Éboli, E. M. Gregores, and F. Halzen, Phys. Lett. B **372**, 127 (1996); **390**, 323 (1997); G. A. Schuler and R. Vogt, *ibid.* **387**, 181 (1996).

[6] E. L. Berger and D. Jones, Phys. Rev. D **23**, 1521 (1981).

[7] R. Baier and R. Rückl, Nucl. Phys. **B201**, 1 (1982).

[8] J. G. Körner, J. Cleymans, M. Kuroda, and G. J. Gounaris, Nucl. Phys. **B204**, 6 (1982); **B213**, 546(E) (1983); Phys. Lett. **114B**, 195 (1982).

[9] M. Krämer, J. Zunft, J. Steegborn, and P. M. Zerwas, Phys. Lett. B **348**, 657 (1995); M. Krämer, Nucl. Phys. **B459**, 3 (1996).

[10] M. Cacciari and M. Krämer, Phys. Rev. Lett. **76**, 4128 (1996).

[11] P. Ko, J. Lee, and H. S. Song, Phys. Rev. D **54**, 4312 (1996).

[12] M. Cacciari and M. Krämer, ''Proceedings of the Workshop on Future Physics at HERA'' [hep-ph/9609500].

[13] F. Maltoni, M. L. Mangano, and A. Petrelli, CERN-TH/97-202 [hep-ph/9708349].

[14] W. Y. Keung and I. J. Muzinich, Phys. Rev. D **27**, 1518 (1983); H. Jung, D. Krücker, C. Greub, and D. Wyler, Z. Phys. C **60**, 721 (1993); G. Schuler, ''Habilitations-schrift,'' CERN-TH.7170/94 [hep-ph/9403387]; H. Khan and P. Hoodbhoy, Phys. Lett. B **382**, 189 (1996).

[15] M. Beneke, I. Z. Rothstein, and M. B. Wise, Phys. Lett. B **708**, 373 (1997).

[16] B. A. Kniehl and G. Kramer, DESY 97-036 [hep-ph/9703280]; Phys. Rev. D **56**, 5820 (1997).

[17] G. P. Lepage, L. Magnea, C. Nakhleh, U. Magnea, and K. Hornbostel, Phys. Rev. D **46**, 4052 (1992).

[18] H1 Collaboration, S. Aid *et al.*, Nucl. Phys. **B472**, 3 (1996); in *ICHEP'96*, Proceedings of the 28th International Conference on High Energy Physics, Warsaw, Poland, 1996, edited by Z. Ajduk and A. Wroblewski (World Scientific, Singapore, 1997).

[19] ZEUS Collaboration, J. Breitweg *et al.*, Z. Phys. C **75**, 215 (1997).

[20] C. Biino *et al.*, Phys. Rev. Lett. **58**, 2523 (1987); C. Akerlof *et al.*, Phys. Rev. D **48**, 5067 (1993); J. G. Heinrich *et al.*, *ibid.* **44**, 1909 (1991).

[21] M. Vänttinen, P. Hoyer, S. J. Brodsky, and W.-K. Tang, Phys. Rev. D **51**, 3332 (1995).

[22] W.-K. Tang and M. Vänttinen, Phys. Rev. D **53**, 4851 (1996); **54**, 4349 (1996).

[23] M. Beneke and I. Z. Rothstein, Phys. Rev. D **54**, 2005 (1996); **54**, 7082(E) (1996).

[24] P. Cho and M. B. Wise, Phys. Lett. B **346**, 129 (1995).

[25] M. Beneke and I. Z. Rothstein, Phys. Lett. B **372**, 157 (1996) **389**, 789(E) (1996).

[26] M. Beneke and M. Krämer, Phys. Rev. D **55**, 5269 (1997).

[27] A. K. Leibovich, Phys. Rev. D **56**, 4412 (1997).

[28] E. Braaten and S. Fleming, Phys. Rev. Lett. **74**, 3327 (1995).

[29] P. Cho and A. K. Leibovich, Phys. Rev. D **53**, 150 (1996); **53**, 6203 (1996).

[30] R. Godbole, D. P. Roy, and K. Sridhar, Phys. Lett. B **373**, 328 (1996).

[31] J. P. Ma, Nucl. Phys. **B498**, 267 (1997).

[32] E. Braaten and Y. Q. Chen, Phys. Rev. D **54**, 3216 (1996).

[33] J. Amundson, S. Fleming, and I. Maksymyk, Phys. Rev. D **56**, 5844 (1997).

[34] M. G. Ryskin, Z. Phys. C **57**, 89 (1993); J. R. Forshaw and M. G. Ryskin, *ibid.* **68**, 137 (1995); M. G. Ryskin, R. G. Roberts, A. D. Martin, and E. M. Levin, *ibid.* **76**, 231 (1997).

[35] S. J. Brodsky, L. Frankfurt, J. F. Gunion, A. H. Mueller, and M. Strikman, Phys. Rev. D **50**, 3134 (1994).

[36] A. Donnachie and P. V. Landshoff, Phys. Lett. B **185**, 403 (1987); **348**, 213 (1995); J. R. Cudell, Nucl. Phys. **B336**, 1 (1990).

[37] M. Binkley *et al.*, Phys. Rev. Lett. **48**, 73 (1982).

[38] ZEUS Collaboration, J. Breitweg *et al.*, Z. Phys. C **76**, 599 (1997).

[39] S. Fleming, O. F. Hernandez, I. Maksymyk, and H. Nadeau, Phys. Rev. D **55**, 4098 (1997).

[40] L. Bergström and P. Ernström, Phys. Lett. B **328**, 153 (1994).

[41] M. Glück, E. Reya, and A. Vogt, Phys. Rev. D **46**, 1973 (1992); Z. Phys. C **67**, 433 (1995).

[42] A. Vogt, Phys. Lett. B **354**, 145 (1995).

[43] A. D. Martin, R. G. Roberts, and W. J. Stirling, Phys. Lett. B **387**, 419 (1996).

[44] S. Fleming and T. Mehen, Phys. Rev. D (to be published).

[45] C. S. Lam and W.-K. Tung, Phys. Rev. D **18**, 2447 (1978).